J. Fluid Mech. (1994), *vol.* 264, *pp.* 107–135

Wall imperfections as a triggering mechanism for Stokes-layer transition

By P. BLONDEAUX AND G. VITTORI
Hydraulic Institute, University of Genoa, Via Montallegro 1, 16145 Genoa, Italy

(Received 26 September 1991 and in revised form 27 September 1993)

The boundary layer generated by the harmonic oscillations of a wavy wall in a fluid otherwise at rest is studied. First the wall waviness is assumed to be of small amplitude and large values of the Reynolds number are considered. The results obtained by means of a linear analysis, where the time variable appears only as a parameter, show that resonance may occur. Indeed it is found that when the Reynolds number is larger than a critical value, an instant within the decelerating part of the cycle exists such that a waviness of infinitesimal amplitude induces unbounded perturbations of the flow in the Stokes layer. The passage through resonance is then studied by means of a multiple-timescale approach, taking into account the damping effect of local acceleration within a small time range around resonance. The asymptotic approach fails beyond a threshold value of the Reynolds number, because the damping effect of the local acceleration terms spreads over the whole cycle. The problem is then tackled by means of an approach that takes into account the above damping effect throughout the whole cycle. Finally, a numerical procedure is used that also allows the inclusion of nonlinear terms and the study of the interactions among forced and free modes. The numerical approach reveals that, even for relatively large values of the amplitude of the wall waviness, nonlinear effects are negligible and the damping of resonance is mainly due to local acceleration effects. The relevance of the results to the understanding of transition to turbulence in Stokes layers is discussed.

1. Introduction

The boundary layer generated by the harmonic oscillations of a fluid parallel to an infinite fixed plate, or conversely by the oscillations of a plate in a fluid otherwise at rest, being a prototype oscillatory boundary layer, has received considerable attention.

The case of a flat plate has been extensively studied since Stokes (1855) determined an exact solution of the Navier–Stokes equations. Since then many experimental, theoretical and numerical studies have been devoted to the study of transition from the laminar to the turbulent regime and of the turbulent characteristics of this flow.

On the experimental side, Li (1954) examined the boundary layer close to an oscillating plate and claimed, using visual means, that the critical value of the Reynolds number for transition to turbulence is 565. The Reynolds number R_δ is defined as $U_0^* \delta^*/\nu$, U_0^* and ω^* being the amplitude and the angular frequency of the velocity oscillations of the plate, ν the kinematic viscosity of the fluid and δ^* the characteristic viscous length $(2\nu/\omega^*)^{\frac{1}{2}}$.

Sergeev (1966), Merkly & Thomann (1975), Hino, Sawamoto & Takasu (1976) and Eckmann & Grotberg (1991) examined transition in oscillatory pipe flow. Sergeev (1966) used both visual means and measurements of the power input to the driving motor to assess transition. In a series of experiments he found a critical Reynolds number of about 500. Merkly & Thomann (1975) found that perturbations to the laminar flow are present when the Reynolds number is larger than a value approximately equal to 280. Moreover, they observed that turbulence occurs in the form of periodic bursts which are followed by relaminarization within the same cycle and did not observe any case in which turbulence occurred throughout the whole cycle. Hino *et al.* (1976) found that disturbances of the laminar flow first appear at Reynolds numbers in the range 70–550 depending on the ratio r between the thickness of the Stokes boundary layer and the radius of the pipe, provided the latter is not too small. However, they found that the velocity profiles exhibit only small deviations from the laminar case. On the contrary when the Reynolds number exceeds 550, for every value of r except for very small values, the velocity profiles are disturbed by fluctuations which are much larger than those characterizing the previous regime. In this situation laminar perturbations appear only in the decelerating phases while in the accelerating phases the flow recovers laminar-like features. Thus this Reynolds-number regime was described by Hino *et al.* (1976) as 'conditional turbulence'. Finally Hino *et al.* (1976) introduced the term 'fully turbulent' to describe states where perturbations are present both in the accelerating and decelerating phases. However, they were unable to observe such a regime. Ramaprian & Muller (1980) carried out experiments at a fixed value of the Reynolds number (namely 370) hence they could not identify a critical value for transition. They found that at the above Reynolds number disturbances are present, but defined the flow as 'transitional' rather than turbulent. Indeed the flow exhibited velocity distributions only mildly different from those predicted by the laminar theory, although the presence of turbulence activity could be inferred from the instantaneous velocity signal. Also Tromans (1976) detected different levels of turbulence. He found a critical value of the Reynolds number for the onset of instability equal to 130 and a value equal to 500 above which he observed what he defined as the turbulent regime. As in Merkly & Thomann's (1975) experiment Tromans found that turbulence appears only during decelerating phases, while in the accelerating phases the flow recovers a laminar behaviour. More recently Eckmann & Grotberg (1991) detected transition to turbulence at R_δ equal to 500 and found turbulence only during decelerating phases of the motion confined to an annular region near the pipe wall. Finally, Monkewitz & Bunster (1985) observed that the laminar Stokes profile shows no significant distortion up to values of the Reynolds number of approximately 500. Moreover they found that a vortical disturbance appeared very clearly at a Reynolds number equal to 647 just before flow reversal.

From the picture emerging from experimental observations one may conclude that for values of the Reynolds number ranging from the laminar to the fully developed turbulent regime characterized by turbulence present throughout the cycle, two other broad flow regimes can be identified:

(i) a disturbed laminar regime, where 'small-amplitude' perturbations appear superimposed on the Stokes flow,

(ii) an intermittently turbulent flow, where bursts of turbulence appear explosively only during the decelerating phases of the cycle.

The former regime takes place for values of the Reynolds number R_δ falling approximately within the range 100–500. The latter regime appears for R_δ larger than about 500 but smaller than a value which has not been experimentally determined yet.

On the theoretical side Von Kerczek & Davis (1974) and Hall (1978) performed linear stability analyses of 'finite' and 'infinite' Stokes layers. They found the flow to be stable within the investigated range of the Reynolds number. Von Kerczek & Davis

(1974) for the finite case and later Blondeaux & Seminara (1979) for the infinite case adopted a 'momentary' criterion for instability and found that for R_δ larger than 86 there are parts of the cycle near flow reversal during which the flow is unstable. Parts of the cycle within which the flow turns out to be unstable were also shown by Tromans (1976), Monkewitz (1983) and Cowley (1987).

More recently Akhavan, Kamm & Shapiro (1991) studied the time development of disturbances of Stokes flow both of infinitesimal and finite amplitude by means of the numerical simulation of Navier–Stokes and continuity equations. In accordance with the analyses of Von Kerczek & Davis (1974) and Hall (1978), all infinitesimal disturbances were found to decay. However, infinitesimal three-dimensional disturbances were found to grow when interacting with pre-existing finite-amplitude two-dimensional waves. Akhavan *et al.* (1991) tried to explain this numerical finding using ideas developed by Pierrehumbert (1986), Bayly (1986) and Landman & Saffman (1987) in different contexts. In the latter works it is shown that in many shear flows the existence of two-dimensional finite-amplitude waves leads to vortical structures within the flow which in approximate form can locally be described by elliptical streamlines. These local eddy flows turn out to be unstable with respect to three-dimensional perturbations, the growth of which may lead to turbulence. This instability mechanism was found to be effective in a wide class of wall-bounded shear flows, including plane and pipe Poiseuille flows, Couette flow and flat-plate boundary layers (Bayly, Orszag & Herbert 1988). It is worth pointing out that the instability mechanism of shear flows described in the above works depends critically on the existence of two-dimensional linearly unstable disturbances, the time development of which because of nonlinear effects leads asymptotically to finite-amplitude waves. On the other hand the above mechanism is independent of the details of the basic flow.

From the results of Akhavan *et al.* (1991), it thus appears that the presence of two-dimensional waves of finite amplitude is crucial in triggering transition to turbulence. The momentary instability of the Stokes layer predicted on the basis of a linear analysis (Von Kerczek & Davis 1974; Blondeaux & Seminara 1979) does not provide a full justification for the existence of the finite-amplitude waves necessary to trigger the explosive growth of three-dimensional perturbations. Indeed in accordance with the results by Von Kerczek & Davis (1974) and Hall (1978), two-dimensional perturbations of small amplitude are found by Ahkavan *et al.* (1991) to experience a net decay over a cycle and, if present, they would disappear after few cycles.

With this in mind, we study the two-dimensional viscous oscillatory flow over a wavy wall of small amplitude to see if small imperfections of the wall may induce large flow perturbations and trigger transition to turbulence.

While the present work was in progress, a possible mechanism for the generation of large-amplitude perturbations in a flat Stokes layer was pointed out by Wu (1992), who considered the nonlinear evolution of a high-frequency inviscid disturbance, composed of a two-dimensional wave and a pair of oblique waves. He showed that the amplitudes of the three waves can develop a finite-time singularity, the explosive growth being induced by nonlinear interactions inside critical layers. In the inviscid analysis by Wu (1992), R_δ is required to be much larger than the inverse of the dimensionless amplitude of the perturbations. It follows that when the initial amplitude of the perturbation is very small, extremely large values of R_δ are considered or conversely for a fixed value of R_δ only perturbations characterized by relatively large values of the initial amplitudes can be analysed. One of the referees has pointed out that recently Wu, Lee & Cowley (1993) and Wu & Cowley (1994), in one as yet unpublished paper, have also considered viscous effects which, for large values of the Reynolds number, were found to become important first in the critical layers far from the wall and then in the wall layer.

In the present work it is shown that an aperiodic flow with many characteristics in common with the bursting turbulent flow detected experimentally in Stokes layers, can be generated even in the two-dimensional case by the interaction among the momentarily unstable modes predicted by Blondeaux & Seminara (1979) and the forced modes induced by wall imperfections.

Many works have been devoted to the study of the Stokes flow over a plate characterized by the presence of a small-amplitude waviness. Lyne (1971) studied the viscous boundary layer induced by fluid oscillations near a wall characterized by presence of a two-dimensional waviness of amplitude ϵ^* much smaller than the characteristic viscous length δ^*. Moreover he restricted his attention to small or large values of the ratio K between the amplitude of fluid displacement oscillations a^* and the wavelength l^* of the wall waviness. These asymptotic values of K were also considered by Sleath (1976). Later Kaneko & Honji (1979) extended Lyne's theory by considering higher-order solutions in the parameters ϵ^*/δ^* and a^*/l^*. More recently Blondeaux (1990) and Hara & Mei (1990) determined the oscillatory flow over a two-dimensional wavy wall for values of K of order one, assuming infinitesimal values of ϵ^*/δ^* and of ϵ^*/l^* respectively. Finally Vittori (1988) extended these works by considering values of a^*/l^* of order one but including nonlinear effects in the parameter ϵ^*/δ^* and considering three-dimensional wall profiles of small amplitude (Vittori 1992). However, none of the above works can provide an explanation for the presence of large perturbations of the Stokes flow since all the above analyses find corrections of the Stokes flow which scale with the amplitude of the wall waviness, which is assumed infinitesimal.

Here we study the viscous oscillatory flow over a two-dimensional wall waviness of small amplitude with the further assumption of large values of the parameter K, the ratio between the amplitude of fluid oscillations and the wavelength of wall waviness. This problem has already been tackled by Lyne (1971) who focused his attention only on wavelengths much larger than the boundary-layer thickness δ^*. In contrast we consider wavelengths of the same order of magnitude as δ^*. Taking into account that K is equal to $\frac{1}{2}R_\delta(\delta^*/l^*)$, the analysis is carried out for δ^*/l^* of order one and large values of R_δ. The present results show that for δ^*/l^* of order one, resonance may occur. Indeed, using a linear scheme and neglecting terms of $O(1/K)$, it is found that when the Reynolds number is larger than a critical value, an instant within the decelerating parts of the cycle exists in which an infinitesimal wall waviness, characterized by a wavelength which depends on R_δ, induces perturbations in the Stokes flow which turn out to develop an infinite peak. At this stage the only requirements of the analysis are $\epsilon \ll 1$ and $R_\delta \gg 1$. The infinite peak can then be removed, including the effects of the local acceleration which, for sufficiently small values of ϵ, are more important than nonlinear effects. For moderate values of R_δ the bounded amplitude of the perturbations can be determined by means of a multiple-timescale approach (Kevorkian 1971), which takes into account the damping effect of the local acceleration term only within a small time range around resonance. However, on increasing the Reynolds number, the asymptotic approach fails because the local acceleration effects spread over the whole cycle. The problem can then be tackled by means of the approach described in Blondeaux (1990), which however becomes computationally heavier for increasing values of R_δ. Thus a numerical procedure should finally be used. The use of a numerical procedure also allows the inclusion of the nonlinear terms and the study of the interaction among the flow perturbations forced in the Stokes flow by the wall waviness and the free modes studied by Blondeaux & Seminara (1979).

A contribution is thus made to boundary receptivity studies, where the effects of non-localized irregularities are investigated (for a review of the effects of localized disturbances, the interested reader is referred to Goldstein & Hultgren 1989). Experiments on the Blasius boundary layer by Corke, Bar Sever & Morkovin (1986) and Reshotko (1984) show that wall roughness can be a source of short-wave disturbances. In the above investigations a steady free stream was considered, so that the roughness is expected to induce only stationary disturbances. These disturbances, however, (Reshotko 1984) are involved in the development of the travelling eigenmodes. More recently Crouch (1992) has presented an analysis for the acoustic receptivity of Blasius boundary layers over a surface characterized by a small waviness. However, the free stream is assumed to be the sum of a steady term plus an acoustic wave of small amplitude.

Interesting results are found in the present contribution where a pure oscillatory external flow is considered. Indeed by means of the numerical procedure it is found that even when neglecting three-dimensional effects the oscillatory flow over a wavy wall is characterized by bursts of an aperiodic motion which take place during the decelerating parts of the cycle and can be interpreted as the onset of turbulence.

The structure of the rest of the paper is the following. In the next section we formulate the problem. The solution procedure is presented in §3 along with the results which show the existence of the resonance previously outlined. In §4 the passage through resonance is studied by means of both a multiple-scale technique and by a numerical approach. The relevance of the work in explaining transition in the Stokes boundary layer is discussed in the final section.

2. Formulation of the problem

Let us consider a wavy wall bounding a viscous fluid of density ρ and kinematic viscosity ν. We refer to a fixed Cartesian coordinate system (x^*, y^*) and describe the wall profile by the following relationship:

$$y^* = \epsilon^* \eta_1(x^*, t^*) = \epsilon^* \exp\left[\mathrm{i}\alpha^*\left(x^* - \int_0^{t^*} u^*(t^*)\,\mathrm{d}t^*\right) + \text{c.c.}\right], \tag{1}$$

where c.c. denotes the complex conjugate of a complex number.

It is easy to see that (1) represents a wavy wall of amplitude $2\epsilon^*$ and wavenumber α^* oscillating in the x^* direction with velocity $u^*(t^*)$. We assume

$$u^*(t^*) = \tfrac{1}{2} U_0^* \left(\mathrm{e}^{\mathrm{i}\omega^* t^*} + \text{c.c.}\right), \tag{2}$$

where U_0^* and ω^* are the amplitude and the angular frequency of the velocity oscillations of the wall.

The flow induced in the fluid by the wall oscillations is described in terms of the stream function by the vorticity equation and boundary conditions which force no-slip at the wall and decay of the flow far from the wall.

Introducing the following dimensionless variables:

$$(x, y, \epsilon, \alpha^{-1}) = (x^*, y^*, \epsilon^*, \alpha^{*-1})/\delta^*, \quad t = t^*\omega^*, \quad \psi = \psi^*/U_0^*\delta^*, \tag{3}$$

where $\delta^* = (2\nu/\omega^*)^{\frac{1}{2}}$ is the conventional thickness of Stokes boundary layer, the flow problem becomes

$$\frac{2}{R_\delta}\frac{\partial}{\partial t}(\nabla^2\psi)+\frac{\partial\psi}{\partial y}\frac{\partial}{\partial x}(\nabla^2\psi)-\frac{\partial\psi}{\partial x}\frac{\partial}{\partial y}(\nabla^2\psi)=\frac{1}{R_\delta}\nabla^4\psi, \tag{4}$$

$$\frac{\partial\psi}{\partial x}=0,\quad \frac{\partial\psi}{\partial y}=\tfrac{1}{2}\mathrm{e}^{\mathrm{i}t}+\text{c.c.}\quad \text{at}\quad y=\epsilon\eta_1, \tag{5}$$

$$\frac{\partial\psi}{\partial x}\to 0,\quad \frac{\partial\psi}{\partial y}\to 0\quad \text{for}\quad y\to\infty. \tag{6}$$

Herein the Reynolds number R_δ is defined as $U_0^*\,\delta^*/\nu$.

3. Linear analysis

3.1. *The solution*

Assuming ϵ to be small, it is feasible to expand the forced solution in powers of ϵ. Moreover, because at order one the wall turns out to be plane, the leading-order term of the stream function will be taken to be independent of x, hence

$$\psi(x,y,t)=\psi_0(y,t)+\epsilon\psi_1(x,y,t)+O(\epsilon^2). \tag{7}$$

Substituting from (7) into (4), (6) and equating like powers of ϵ, differential equations are obtained at the various orders of approximation which are examined in sequence.

At order one the Stokes solution is readily obtained:

$$\psi_0(y,t)=F_0(y)\,\mathrm{e}^{\mathrm{i}t}+\text{c.c.}=\frac{1}{2}\left[\frac{-1}{1+\mathrm{i}}\mathrm{e}^{-(1+\mathrm{i})\,y}\right]\mathrm{e}^{\mathrm{i}t}+\text{c.c.} \tag{8}$$

At order ϵ^1 the following equation is found:

$$\frac{2}{R_\delta}\frac{\partial}{\partial t}(\nabla^2\psi_1)+\frac{\partial\psi_0}{\partial y}\frac{\partial}{\partial x}(\nabla^2\psi_1)-\frac{\partial\psi_1}{\partial x}\frac{\partial}{\partial y}(\nabla^2\psi_0)=\frac{1}{R_\delta}\nabla^4\psi_1, \tag{9}$$

along with the boundary conditions which come from the no-slip condition at the wall and the matching of the flow with the fluid at rest far from the wall

$$\frac{\partial\psi_1}{\partial x}=0,\quad \frac{\partial\psi_1}{\partial y}=-\frac{\partial^2\psi_0}{\partial y^2}\eta_1\quad \text{at}\quad y=0, \tag{10a, b}$$

$$\frac{\partial\psi_1}{\partial x}\to 0,\quad \frac{\partial\psi_1}{\partial y}\to 0,\quad \text{for}\quad y\to\infty. \tag{11a, b}$$

Considering large values of the Reynolds number R_δ, the solution can be expanded in the form

$$\psi_1(x,y,t)=\left[\phi_0(y,t)+O\left(\frac{1}{R_\delta}\right)\right]P(t)\,\mathrm{e}^{\mathrm{i}\alpha x}+\text{c.c.}, \tag{12}$$

where
$$P(t)=\exp\left[-\tfrac{1}{2}\mathrm{i}\alpha R_\delta\int_0^t u(t)\,\mathrm{d}t\right]. \tag{13}$$

At the leading order of approximation in the parameter R_δ^{-1}, substitution from (12) and (13) into (9)–(11) leads to the classical Orr–Sommerfeld equation with non-homogeneous boundary conditions

$$\left(\frac{\partial \psi_0}{\partial y}-u(t)\right)\mathrm{N}^2\phi_0-\phi_0\frac{\partial^3\psi_0}{\partial y^3}=\frac{1}{\mathrm{i}\alpha R_\delta}\mathrm{N}^4\phi_0, \tag{14}$$

$$\phi_0=0,\quad \frac{\partial \phi_0}{\partial y}=-\frac{\partial^2\psi_0}{\partial y^2}\quad \text{at}\quad y=0. \tag{15}$$

$$\phi_0\rightarrow 0,\quad \frac{\partial \phi_0}{\partial y}\rightarrow 0\quad \text{for}\quad y\rightarrow\infty, \tag{16}$$

where the operator N^2 is defined by

$$\mathrm{N}^2\equiv\frac{\partial^2}{\partial y^2}-\alpha^2. \tag{17}$$

In (14) the viscous term is retained since it turns out to be significant at leading order in a viscous layer close to the wall, the thickness of which is of order $R_\delta^{-\frac{1}{3}}$ and within critical layers where $\partial\psi_0(y,t)/\partial y$ equals the plate velocity $u(t)$. A more formal approach would first require the solution of the inviscid version of (14). The latter is singular for values of y such that $\partial\psi_0(y,t)/\partial y=u(t)$. Hence in critical layers close to such singular planes viscous terms should be retained. The inviscid solution should then be matched with the solutions in the critical layers. Such a procedure would involve a lot of tedious and heavy algebra. The direct solution of the problem (14)–(16) has thus been preferred.

In the Appendix it is shown that, for values of t around $n\pi$ when the wall critical layer is the only one, the solution of (14) coincides, to the required order of approximation, with the solution obtained on the basis of a matched asymptotic approach. It is also worth pointing out that the numerical solution of the problem, where the fluid domain is split into an inviscid region and viscous layers, provides results coincident to the order required with those obtained by the solution described below.

We may note that the time variable t appears only as a parameter in (14). This is because of our insistence on a periodic solution with the same angular frequency of the forcing term which implies that $(\partial/\partial t)\sim O(1)$ and hence $(2/R_\delta)(\partial/\partial t)\ll 1$.

Equation (14) can be solved at each instant of time in terms of a double series expansion based on the following constructive procedure developed by Seminara & Hall (1976) and used in a similar context by Blondeaux & Seminara (1979). In the absence of the convective terms, (14) has two solutions which, for large values of y, decay, being proportional to $\mathrm{e}^{-\alpha y}$ and to $\mathrm{e}^{-\sigma y}$ $(\sigma(t)=[\alpha^2-\mathrm{i}\alpha R_\delta u(t)]^{\frac{1}{2}})$. Since each of these basic solutions interacts with the basic flow, an infinite sequence of terms is required in the final solution in order to achieve an appropriate balance. Thus one is led to the following form of the solution:

$$\phi_0(y,t)=\sum_{n=0}^{\infty}\sum_{m=0}^{n}a_{n,m}^{(0)}(t)\exp\{-[\alpha+n(1+\mathrm{i})-2\mathrm{i}m]y\}$$
$$+\sum_{n=0}^{\infty}\sum_{m=0}^{n}b_{n,m}^{(0)}(t)\exp\{-[\sigma+n(1+\mathrm{i})-2\mathrm{i}m]y\}. \tag{18}$$

The coefficients $a^{(0)}_{n,m}$ are expresed in terms of $a^{(0)}_{0,0}$ through recursive relationships, which are obtained by forcing (18) to satisfy (14); hence

$$a^{(0)}_{n,m} = \frac{\frac{1}{2}\mathrm{i}\alpha R_\delta[\lambda_1 \mathrm{e}^{\mathrm{i}t}(\chi^2_{n-1,m}-\alpha^2-2\mathrm{i})\,a^{(0)}_{n-1,m}+\lambda_2 \mathrm{e}^{-\mathrm{i}t}(\chi^2_{n-1,m-1}-\alpha^2+2\mathrm{i})\,a^{(0)}_{n-1,m-1}]}{\chi^4_{n,m}-2\alpha^2\chi^2_{n,m}+\alpha^4+\mathrm{i}\alpha R_\delta u(t)(\chi^2_{n,m}-\alpha^2)}, \quad (19)$$

where

$$\lambda_1 = \begin{cases} 0, & m=n \\ 1, & 0 \leqslant m \leqslant n-1, \end{cases} \quad \lambda_2 = \begin{cases} 0, & m=0 \\ 1, & 1 \leqslant m \leqslant n, \end{cases} \quad \chi_{n,m} = -[\alpha+n(1+\mathrm{i})-2\mathrm{i}m].$$

Similarly the coefficients $b^{(0)}_{n,m}$ can be expressed in terms of $b^{(0)}_{0,0}$ through relationships analogous to (19) where $\chi_{n,m}$ are replaced by $\theta_{n,m}$ which is the quantity $(-[\sigma+n(1+\mathrm{i})-2\mathrm{i}m])$.

We note that the solution (18) vanishes at infinity as required by boundary conditions (6) while the no-slip condition at the wall leads to the following algebraic linear system for $a^{(0)}_{0,0}$ and $b^{(0)}_{0,0}$:

$$\left.\begin{aligned} &a^{(0)}_{0,0}\sum_{n=0}^{\infty}\sum_{m=0}^{n}(a^{(0)}_{n,m}/a^{(0)}_{0,0})+b^{(0)}_{0,0}\sum_{n=0}^{\infty}\sum_{m=0}^{n}(b^{(0)}_{n,m}/b^{(0)}_{0,0}) = 0, \\ &a^{(0)}_{0,0}\sum_{n=0}^{\infty}\sum_{m=0}^{n}(a^{(0)}_{n,m}/a^{(0)}_{0,0})\,\chi_{n,m}+b^{(0)}_{0,0}\sum_{n=0}^{\infty}\sum_{m=0}^{n}(b^{(0)}_{n,m}/b^{(0)}_{0,0})\,\theta_{n,m} = \tfrac{1}{2}(1+\mathrm{i})\,\mathrm{e}^{\mathrm{i}t}+\text{c.c.}, \end{aligned}\right\} \quad (20)$$

which allows the flow to be completely determined.

The solution of system (20) requires a relative modest numerical effort, even for large values of the Reynolds number when the number of terms which must be retained in the expansion (18) is relatively large. Indeed the inversion of a 2×2 matrix can be easily performed and the evaluation of the coefficients $a^{(0)}_{n,m}, b^{(0)}_{n,m}$ does not lead to a prohibitive amount of computation. At this stage it is useful to point out that the series expansions (18) are truncated at $n = N_1$. Numerical experiments showed that satisfactory convergence is achieved for values of N_1 that increase as R_δ increases. However the values of N_1, for the range of R_δ of interest, are relatively small.

At flow reversal when $u(t)$ vanishes, (18) ceases to be valid. Indeed $\sigma(t)$ is found to be equal to α and the two independent solutions $\mathrm{e}^{-\alpha y}$ and $\mathrm{e}^{-\sigma y}$, which have been found by neglecting convective terms, become $\mathrm{e}^{-\alpha y}$ and $y\mathrm{e}^{-\alpha y}$. However, it can be easily verified that at $t = \frac{1}{2}\pi$ and $\frac{3}{2}\pi$ the function ϕ_0 can be expressed in the following form:

$$\phi_0(y,t) = \sum_{n=0}^{\infty}\sum_{m=0}^{n} c_{n,m}(t)\exp\{-[\alpha+n(1+\mathrm{i})-2\mathrm{i}m]\,y\} + \sum_{n=0}^{\infty}\sum_{m=0}^{n} y d_{n,m}(t)\exp\{-[\alpha+n(1+\mathrm{i})-2\mathrm{i}m]\,y\}, \quad (21)$$

where the coefficients $c_{n,m}$ and $d_{n,m}$ can be evaluated by means of recursive relationships similar to (19) and the values of $c_{0,0}$ and $d_{0,0}$ can be determined solving an algebraic linear system similar to (20). It is worth pointing out that the solution turns out to be continuous since (18) tends to (21) when t approaches $\frac{1}{2}\pi$ and $\frac{3}{2}\pi$.

3.2. *Results*

As pointed out in the introduction, the boundary layer generated by the harmonic oscillations of a fluid adjacent to a fixed wavy plate has received considerable attention. We have mentioned above some of the works on the subject where different ranges of

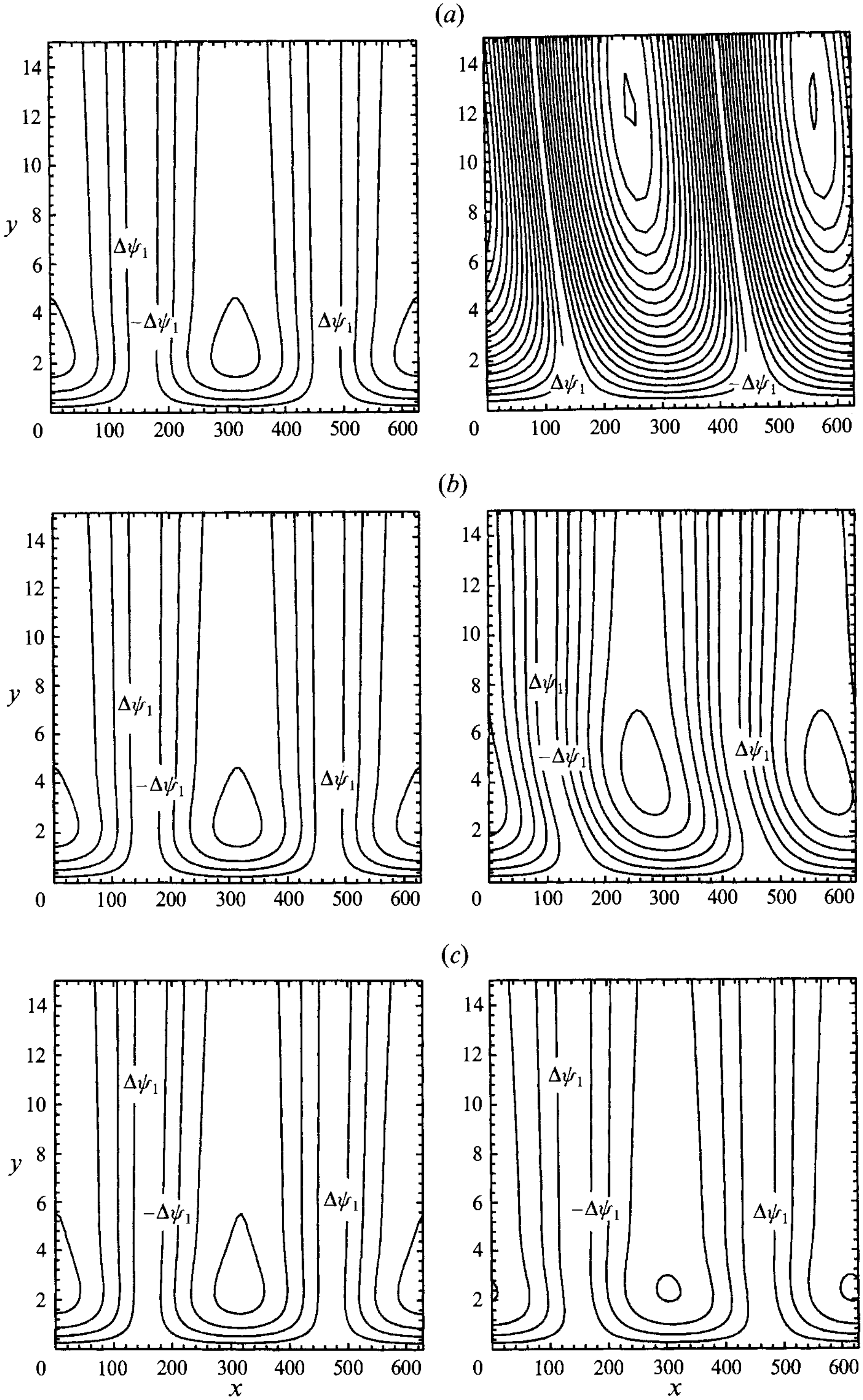

FIGURE 1. Spatial structure of the correction to the stream function induced by a wall waviness in the Stokes flow ($\psi_1(x, y, t)$): $\alpha = 0.01$, $t = 0$. (*a*) $R_\delta = 5$, (*b*) $R_\delta = 50$, (*c*) $R_\delta = 500$. Left-hand plots: analytical results of Blondeaux (1990) ($\Delta\psi_1 = 0.48$). Right-hand plots: results ($\Delta\psi_1 = 0.48$).

the parameters have been analysed. In particular Lyne (1971) assumed the amplitude of the wall waviness to be much smaller than δ^* and considered large values of K ($K = \alpha R_\delta/4\pi$) and wavenumbers α such that $\alpha \sim O(R_\delta)^{-\frac{1}{3}}$.

Similarly the present solution holds for small values of ϵ and large values of R_δ, but it considers values of α of order one. The investigation of the range $\alpha = O(1)$ has shown the existence of a resonance effect in the oscillatory flow over a wavy wall. Indeed the Stokes flow is modified, owing to the presence of a wall waviness, by the term $[\epsilon P(t)\,\phi_0(y,t)\,\mathrm{e}^{\mathrm{i}\alpha x}+\mathrm{c.c.}]$ plus corrections of order $(\epsilon^2, \epsilon/R_\delta)$. The function ϕ_0 is given by (18) and is finite when the determinant D of the system (20) does not vanish. When D approaches zero, $a^{(0)}_{0,0}$ and $b^{(0)}_{0,0}$ tend to infinity and the correction of the Stokes flow is no longer bounded: resonance occurs, i.e. wall waviness triggers a natural response of the system.

Before discussing in detail this resonance effect, let us look at the results related to the case when D does not vanish and analyse them for values of the parameters that allow a comparison with previous analyses. The fact that α is of order one means that the results of Vittori (1988) and Blondeaux (1990) can be used as a check. However, this comparison can be performed only for fairly large values of R_δ or conversely for quite large R_δ but small α since the approaches by Vittori (1988) and Blondeaux (1990) become too expensive for αR_δ larger than values ranging from about 10. In figure 1 the correction to the Stokes flow induced by the waviness is shown in the (x,y)-plane at the same instant within the cycle for fixed α and for different values of the Reynolds number. In the left-hand plots results obtained by means of the approach described in Blondeaux (1990) are shown, while the present results are plotted in the right-hand plots. Incidentally we point out that the approach described in Vittori (1988) provides results practically coincident with those of Blondeaux (1990). The present solution is quite different from that of Blondeaux (1990) when $R_\delta = 5$, but they tend to agree, as expected, when larger values of R_δ are considered. For $R_\delta = 500$ the two solutions are almost coincident. Similar results are found for other values of the parameters.

As previously pointed out, the present solution allows us to obtain results for values of α of order one and large R_δ when other approaches fail. In figure 2 the spatial structure of the correction to the Stokes flow is shown at $t = 0$ for different values of α when $R_\delta = 250$. According to Vittori's (1988) findings only two recirculating cells within a wavelength are found, R_δ being large and α of order one (see figure 8 of Vittori 1988). Looking at figure 2, it is necessary to recall that solution (18) can be split into two parts: the former related to the values of α and of the coefficients $a^{(0)}_{n,m}$, the latter related to the values of $\sigma(t) = [\alpha^2 - \mathrm{i}\alpha R_\delta u(t)]^{\frac{1}{2}}$ and of the coefficients $b^{(0)}_{n,m}$. Increasing α, with R_δ fixed, the two parts decay more rapidly in the y-direction and the two cells appearing in figure 2 decrease in height: the region affected by the waviness turns out to be of the same order of magnitude as its wavelength. When α is kept fixed and R_δ is increased, only σ increases and only the second part of the solution is affected, keeping constant the thickness of the region affected by the wall waviness.

A wider discussion of the influence of α and R_δ is unnecessary in the present context. On the other hand it is of interest to analyse the resonance effect briefly described previously. For particular values of α and R_δ and at particular instant within the cycle, D tends to vanish. It can be easily verified that in this situation wall waviness triggers a natural response of the Stokes flow which is characterized by a timescale δ^*/U^*_0, faster than the basic timescale $2\pi/\omega^*$ when R_δ is large. These free modes of the Stokes flow were analysed by Blondeaux & Seminara (1979), who studied the stability of the Stokes layer using a 'momentary' criterion for instability of the kind introduced by Shen (1961) and discussed by Seminara & Hall (1975). Blondeaux & Seminara (1979)

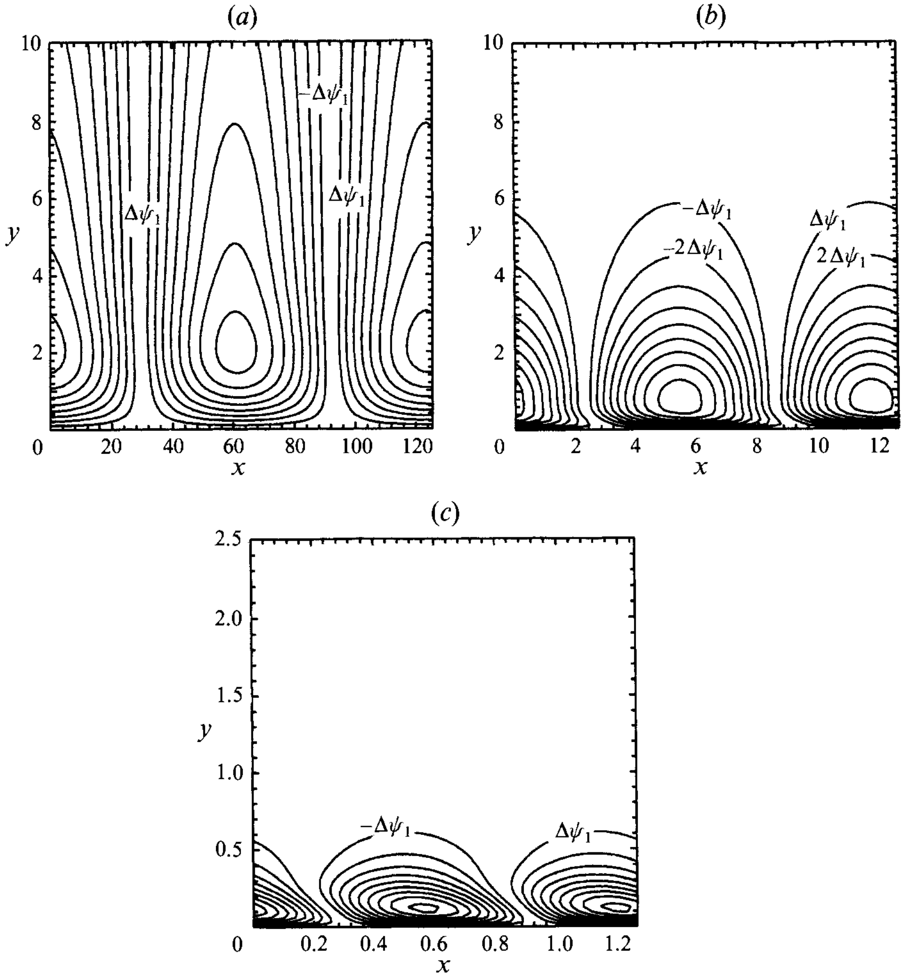

FIGURE 2. Spatial structure of the correction to the stream function induced by a wall waviness in the Stokes flow ($\psi_1(x,y,t)$): $R_\delta = 200$, $t = 0$. (*a*) $\alpha = 0.05$, $\Delta\psi_1 = 0.2$; (*b*) $\alpha = 0.5$, $\Delta\psi_1 = 0.04$; (*c*) $\alpha = 5.0$, $\Delta\psi_1 = 0.01$.

studied the time development of perturbations of infinitesimal amplitude, the stream function of which can be assumed to be of the form

$$\psi = \epsilon\Phi_0(y,t)\exp\left[\mathrm{i}\beta\left(x - R_\delta\int c(t)\,\mathrm{d}t\right)\right] + \text{c.c.} + O(\epsilon R_\delta^{-1}, \epsilon^2), \tag{22}$$

where β is the perturbation wavenumber, the real part (c_r) of c is the wavespeed of the perturbation and the imaginary part (c_i) controls its growth or decay. Substituting (22) into the vorticity equation and using the appropriate boundary conditions, a problem similar to (14)–(16) is found, where the complex growth rate $2c(t)$ replaces the plate velocity $u(t)$ and homogeneous conditions at the wall replace (15). The eigenrelation $f(\beta, R_\delta, t, c) = 0$, which allows values of Φ_0 different from zero, is determined in Blondeaux & Seminara (1979). It is now clear that if values of R_δ, α and t are found such that $\alpha = \beta$, $u(t) = 2c_r(t)$ and $c_i(t) = 0$, the wall waviness triggers a natural response of the system.

An example of the behaviour of c is shown in figure 3 as a function of time for

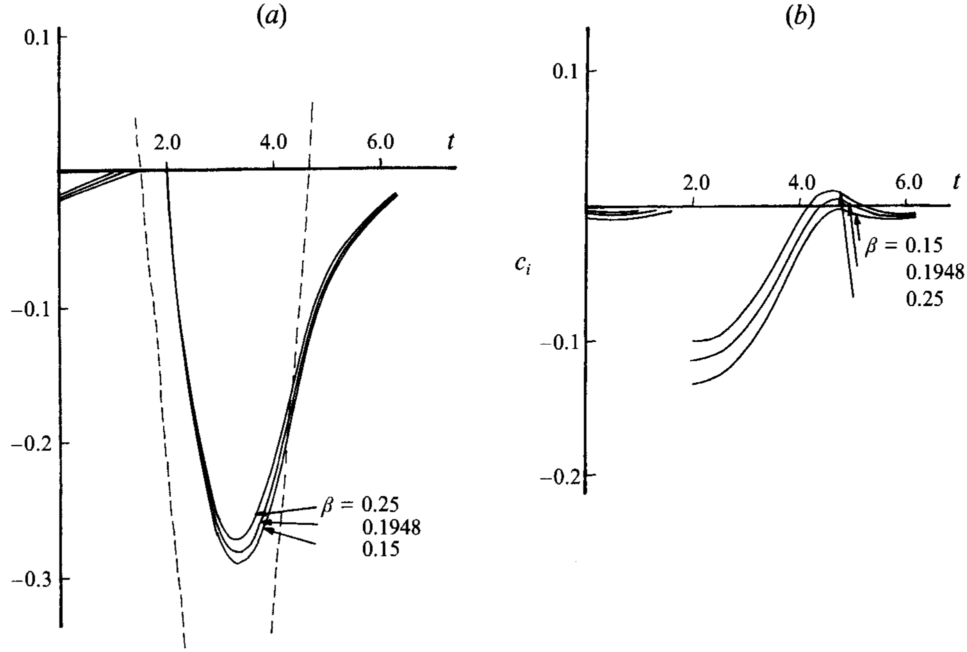

FIGURE 3. The eigenvalue c as function of t for $R_\delta = 200$ and different values of β: (a) real part, (b) imaginary part. The dashed line represents half the wall velocity.

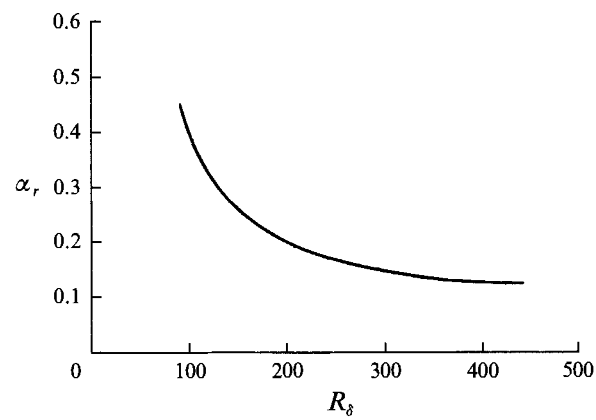

FIGURE 4. The value of α that causes resonance plotted versus R_δ.

$R_\delta = 200$ and different values of β. In figure 3 $\frac{1}{2}u(t)$ is also plotted. For every value of β an instant of time within the cycle exists such that $c_r(t) = \frac{1}{2}u(t)$, but only for a particular value of β does this instant coincide with the instant at which $c_i(t)$ vanishes. For $R_\delta = 200$ it is found that resonance occurs at $t = 1.2188$ when α is equal to about 0.1948.

The values α_r of α that are able to induce resonance are plotted versus R_δ in figure 4, while figure 5 shows the instant t_r within the cycle at which resonance occurs. Since it can be shown that, for a fixed value of β, when $c(t)$ is an eigenvalue $c(t) = -c_r(t+\pi)+ic_i(t+\pi)$ is also an eigenvalue, resonance is present every half-cycle.

It is thus found that when the Reynolds number is larger than a value $(R_\delta)_R$ which is about 100, infinitesimal wall perturbations with a particular wavenumber which

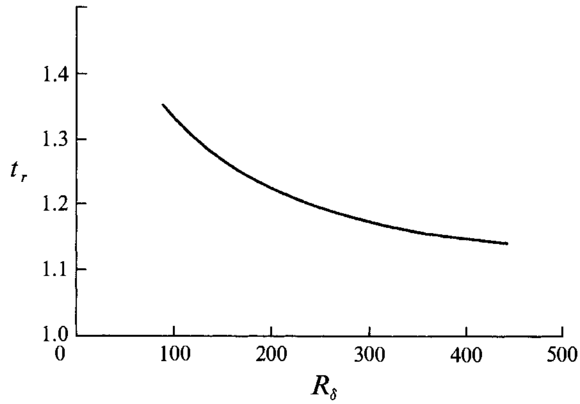

FIGURE 5. The instant within the cycle for which resonance occurs plotted versus R_δ.

depends on R_δ may excite the resonant growth of a spatially synchronous flow mode and induce, during the decelerating parts of the cycles, large modifications of the Stokes flow. In this situation, in order to gain quantitative information on the amplitude of the perturbations of the Stokes flow, the local time derivative term and/or nonlinear terms should be taken into account. In the following section it will be shown that nonlinear effects can be ignored and the local acceleration effects serve to damp the resonant peak.

4. Passage through resonance

4.1. *The asymptotic approach*

Under the assumptions formulated in §§2 and 3, we analyse the flow induced by the oscillations of the wavy wall at resonance, i.e. when R_δ exceeds $(R_\delta)_R$ and α and t differ from α_r and t_r respectively by a small amount which will be defined precisely in the following. There are two possible damping mechanisms that might lead to resonant solutions of bounded amplitude: the former is due to the inclusion of that part of the local acceleration that has been dropped in (9) being negligible far from resonance, the latter is related to the inclusion of nonlinear terms. However, if ϵ is assumed to be much smaller than R_δ^{-1}, after the introduction of a fast timescale τ which scales on some power of R_δ and takes into account the rapid variations of the solution around resonance, the analysis of the problem reveals that the system is governed by a partial differential equation characterized by weak nonlinearities and with coefficients slowly varying in time. As suggested by Kevorkian (1971), in such systems the damping of resonance is due to the local acceleration term and nonlinearities can be ignored.

Let us thus consider the case when the explosive growth of flow perturbations, which is present for t tending to t_r, is inhibited by the presence of the local acceleration of the fluid. As a preliminary we need to estimate the order of magnitude of the amplitude of flow perturbations when R_δ is larger than $(R_\delta)_R$ and (α, t) is in the proximity of (α_r, t_r) and fix the time range within which resonance takes place $((t-t_r) = \tau R_\delta^{-\gamma_2})$. Let us assume the fundamental component of the perturbation to be of order $\epsilon R_\delta^{\gamma_1}$ with γ_1 and γ_2 real exponents to be determined. At the lowest order, the solution should behave like

$$\psi = \psi_0 + \epsilon R_\delta^{\gamma_1} A(\tau)\, P(t)\, \psi_{11}(y, t)\, \mathrm{e}^{\mathrm{i}\alpha x} + \text{c.c.},$$

with A a complex amplitude function to be determined.

At second order the fundamental is reproduced because of the local time derivative, giving rise to secular terms. Hence provided the condition $\gamma_1+\gamma_2-1=0$ is satisfied, the reproduction of the fundamental occurs at the same order ($O(\epsilon)$) at which the forcing effects of the wall waviness appear, and the requirement of suppression of secular terms also leads to suppressing the singular behaviour of the solution predicted by the linear theory. Moreover, in order to get a solution for the amplitude function $A(\tau)$ which decays when $|\tau|$ tends to infinity, i.e. far from resonance, γ_1 is required to be equal to γ_2. Indeed when $\gamma_1=\gamma_2$ the deviation of ψ_0 from the value at t_r gives a contribution at order ϵ which avoids the exponential growing behaviour of $A(\tau)$. It turns out that $\gamma_1=\gamma_2=\frac{1}{2}$ and α may differ from α_r by an amount of order $R_\delta^{-\frac{1}{2}}$, i.e. $\alpha=\alpha_r+R_\delta^{-\frac{1}{2}}\alpha_1$.

Hence we expand the solution in the following form:

$$\psi(y,t)=\psi_0(y,t)+\epsilon[R_\delta^{\frac{1}{2}}A(\tau)\,\psi_{11}(y)+\psi_{12}(y,\tau)+O(R_\delta^{-\frac{1}{2}})]\,\mathrm{e}^{\mathrm{i}\alpha x}+\text{c.c.}+O(\epsilon^2R_\delta), \tag{23}$$

having introduced a fast timescale $\tau=(t-t_r)\,R_\delta^{\frac{1}{2}}$. Substituting (23) into (4)–(6), the following problem is obtained at $O(\epsilon R_\delta^{\frac{1}{2}})$:

$$\left(\frac{\partial\psi_0}{\partial y}-u(t)\right)_{t=t_r}\mathrm{N}_r^2\,\psi_{11}-\psi_{11}\left(\frac{\partial^3\psi_0}{\partial y^3}\right)_{t=t_r}-\frac{1}{\mathrm{i}\alpha_r R_\delta}\mathrm{N}_r^4\,\psi_{11}=0, \tag{24}$$

$$\psi_{11}=0,\quad \frac{\partial\psi_{11}}{\partial y}=0\quad\text{at}\quad y=0, \tag{25}$$

$$\psi_{11}\rightarrow 0,\quad \frac{\partial\psi_{11}}{\partial y}\rightarrow 0\quad\text{for}\quad y\rightarrow\infty, \tag{26}$$

where N_r is simply N with α set equal to α_r.

Again, as previously explained, the viscous term is retained in (24) because it turns out to be relevant close to the wall and within critical layer where $\partial\psi_0(y,t_r)/\partial y$ equals $u(t_r)$.

Because at this order $\alpha=\alpha_r$ and $t=t_r$, a non-trivial solution can be found following the procedure outlined in §3.1. The unknown function ψ_{11} can be determined by a double series expansion similar to (18) and the system providing the constants $a_{0,0}^{(1)}$, $b_{0,0}^{(1)}$ (corresponding to $a_{0,0}^{(0)}$, $b_{0,0}^{(0)}$ appearing in (18)), turns out to be a homogeneous system with a vanishing determinant. The solution is thus determined but for an arbitrary constant which can be incorporated in the amplitude function $A(\tau)$.

At $O(\epsilon)$ the following non-homogeneous problem is obtained:

$$\begin{aligned}&\left(\frac{\partial\psi_0}{\partial y}-u(t)\right)_{t=t_r}\mathrm{N}_r^2\,\psi_{12}-\psi_{12}\left(\frac{\partial^3\psi_0}{\partial y^3}\right)_{t=t_r}-\frac{1}{\mathrm{i}\alpha_r R_\delta}\mathrm{N}_r^4\,\psi_{12}\\&=\left(2\alpha_r\alpha_1\left(\frac{\partial\psi_0}{\partial y}-u(t)\right)\psi_{11}-\frac{\alpha_1}{\mathrm{i}\alpha_r^2R_\delta}\mathrm{N}_r^4\,\psi_{11}\right)_{t=t_r}A-\left(\frac{\partial^2\psi_0}{\partial y\,\partial t}-\frac{\partial u}{\partial t}\right)_{t=t_r}\mathrm{N}_r^2\,\psi_{11}\,A\tau\\&\quad-\left(\frac{\partial^4\psi_0}{\partial y^3\,\partial t}\right)_{t=t_r}\psi_{11}\,A\tau-\frac{2}{\mathrm{i}\alpha}\mathrm{N}_r^2\,\psi_{11}\frac{\mathrm{d}A}{\mathrm{d}\tau},\end{aligned} \tag{27}$$

$$\psi_{12}=0,\quad \frac{\partial\psi_{12}}{\partial y}=-\frac{\partial^2\psi_0}{\partial y^2}\quad\text{at}\quad y=0. \tag{28}$$

$$\psi_{12}\rightarrow 0,\quad \frac{\partial\psi_{12}}{\partial y}\rightarrow 0,\quad\text{for}\quad y\rightarrow\infty. \tag{29}$$

The homogeneous part of the problem (27)–(29) admits a non-trivial solution and a solvability condition must be satisfied (see Coddington & Levison 1955, p. 294). The analytical approach previously described to find ψ_{11} provides a convenient way to force such a solvability condition and can be used to determine ψ_{12}. Indeed a particular solution $\psi_{12}^{(p)}$ of (27) can be found by assuming

$$\psi_{12}^{(p)} = \psi_{121}^{(p)}\frac{\mathrm{d}A}{\mathrm{d}\tau}+\psi_{122}^{(p)}A\tau+\psi_{123}^{(p)}A, \tag{30}$$

and by determining separately $\psi_{12i}^{(p)}(i=1,2,3)$ using an expansion similar to (18).

Once the particular solution $\psi_{12}^{(p)}$ is determined along with the independent solutions

$$\psi_{12}^{(1)} = \sum_{n=0}^{\infty}\sum_{m=0}^{n}\frac{a_{n,m}^{(2)}}{a_{0,0}^{(2)}}\exp\{-[\alpha+n(1+\mathrm{i})-2\mathrm{i}m]y\},$$

$$\psi_{12}^{(2)} = \sum_{n=0}^{\infty}\sum_{m=0}^{n}\frac{b_{n,m}^{(2)}}{b_{0,0}^{(2)}}\exp\{-[\sigma+n(1+\mathrm{i})-2\mathrm{i}m]y\},$$

of the homogeneous problem, the general solution can be obtained in the form

$$\psi_{12} = a_{0,0}^{(2)}\psi_{12}^{(1)}+b_{0,0}^{(2)}\psi_{12}^{(2)}+\psi_{121}^{(p)}\frac{\mathrm{d}A}{\mathrm{d}\tau}+\psi_{122}^{(p)}A\tau+\psi_{123}^{(p)}A, \tag{31}$$

where the constant $a_{0,0}^{(2)}, b_{0,0}^{(2)}$ should be determined to satisfy the boundary conditions at the bottom

$$\left.\begin{aligned} &a_{0,0}^{(2)}\psi_{12}^{(1)}|_{y=0}+b_{0,0}^{(2)}\psi_{12}^{(2)}|_{y=0} = -\psi_{121}^{(p)}|_{y=0}\frac{\mathrm{d}A}{\mathrm{d}\tau}-\psi_{122}^{(p)}|_{y=0}A\tau-\psi_{123}^{(p)}|_{y=0}A,\\ &a_{0,0}^{(2)}\left.\frac{\partial\psi_{12}^{(1)}}{\partial y}\right|_{y=0}+b_{0,0}^{(2)}\left.\frac{\partial\psi_{12}^{(2)}}{\partial y}\right|_{y=0} = -\left.\frac{\partial^2\psi_0}{\partial y^2}\right|_{y=0}-\left.\frac{\partial\psi_{121}^{(p)}}{\partial y}\right|_{y=0}\frac{\mathrm{d}A}{\mathrm{d}\tau}-\left.\frac{\partial\psi_{122}^{(p)}}{\partial y}\right|_{y=0}A\tau-\left.\frac{\partial\psi_{123}^{(p)}}{\partial y}\right|_{y=0}A. \end{aligned}\right\} \tag{32}$$

Because the determinant of system (32) vanishes, a solvability condition should be forced which reads

$$\frac{\mathrm{d}A}{\mathrm{d}\tau}+a\tau A+bA+c = 0, \tag{33}$$

where

$$a = \frac{-\psi_{12}^{(1)}|_{y=0}\left.\frac{\partial\psi_{122}^{(p)}}{\partial y}\right|_{y=0}+\left.\frac{\partial\psi_{12}^{(2)}}{\partial y}\right|_{y=0}\psi_{122}^{(p)}|_{y=0}}{-\psi_{12}^{(1)}|_{y=0}\left.\frac{\partial\psi_{121}^{(p)}}{\partial y}\right|_{y=0}+\left.\frac{\partial\psi_{12}^{(2)}}{\partial y}\right|_{y=0}\psi_{121}^{(p)}|_{y=0}}, \tag{34a}$$

$$b = \frac{-\psi_{12}^{(1)}|_{y=0}\left.\frac{\partial\psi_{123}^{(p)}}{\partial y}\right|_{y=0}+\left.\frac{\partial\psi_{12}^{(2)}}{\partial y}\right|_{y=0}\psi_{123}^{(p)}|_{y=0}}{-\psi_{12}^{(1)}|_{y=0}\left.\frac{\partial\psi_{121}^{(p)}}{\partial y}\right|_{y=0}+\left.\frac{\partial\psi_{12}^{(2)}}{\partial y}\right|_{y=0}\psi_{121}^{(p)}|_{y=0}}, \tag{34b}$$

$$c = \frac{-\psi_{12}^{(1)}|_{y=0}\left.\frac{\partial^2\psi_0}{\partial y^2}\right|_{y=0}}{-\psi_{12}^{(1)}|_{y=0}\left.\frac{\partial\psi_{121}^{(p)}}{\partial y}\right|_{y=0}+\left.\frac{\partial\psi_{12}^{(2)}}{\partial y}\right|_{y=0}\psi_{121}^{(p)}|_{y=0}}. \tag{34c}$$

The term $a\tau A$ in (33) is the 'damping effect' which comes from the deviation of the time-dependent terms from their values at $t = t_r$. The term bA is proportional to α_1 and

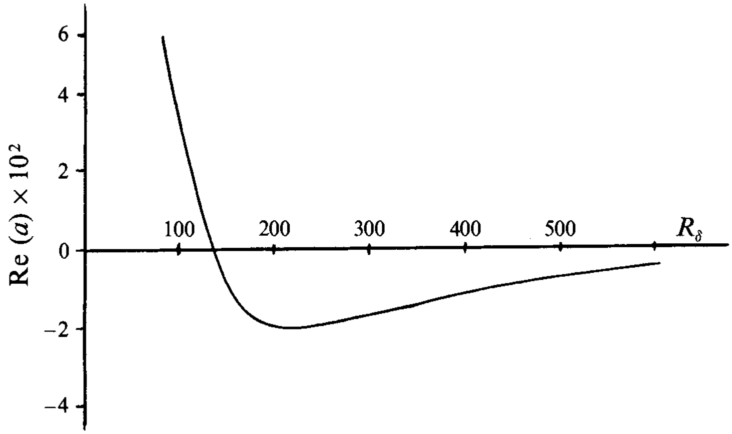

FIGURE 6. The real value of the coefficient a appearing in (34) plotted versus R_δ.

represents the detuning effect which is present when the wall waviness has a wavelength that is not exactly equal to that characteristic of the marginal unstable modes travelling with the wall speed $u(t_r)$. The constant c describes the receptivity mechanism, i.e. the triggering of free modes by the wall waviness.

The solution of (33) is straightforward and reads

$$A = \exp\left[-\tfrac{1}{2}a\tau^2 - b\tau\right]\left\{A_0 - c\int_0^\tau \exp\left[\tfrac{1}{2}a\zeta^2 + b\zeta\right]\mathrm{d}\zeta\right\}. \tag{35}$$

The value of the constant A_0 can then be determined by proper matching with the solution valid far from t_r. Once the solvability condition for the system (32) is forced, ψ_{12} can be obtained but for an amplitude function to be derived at order $\epsilon R_\delta^{-\frac{1}{2}}$. However, this lengthy procedure has not been carried out because this asymptotic approach fails for moderately large values of R_δ.

Indeed (35) turns out to be meaningful only when the real part of a is positive, otherwise A tends to infinity when $|t-t_r|$ increases. When the real part of a is negative, the damping effect of local acceleration cannot be taken into account by means of the multiple-scale approach previously described, because such effect spreads over the whole cycle. Then (9) along with the boundary conditions (10) and (11) should be solved.

As shown in figure 6 the real part of a turns out to be positive only when R_δ is larger than $(R_\delta)_R$ but smaller than 138. To gain some qualitative information on the structure of the solution in this range of R_δ, some examples of the behaviour of $A(\tau)$ are plotted in figure 7 for different values of R_δ and $\alpha_1 = 0$. Because of the equality between α and α_r, the constant A_0 vanishes. In fact at a first order of approximation, the outer solution for t tending to t_r turns out to be odd, thus forcing A_0 to vanish. From the results plotted in figure 7, it appears that within a small time range around resonance, the oscillatory flow over a wavy wall is characterized by large and rapid fluctuations which are also rapidly damped.

As previously pointed out, for R_δ larger than 138, the problem posed by (9) along with boundary conditions (10) and (11) should be solved. In Blondeaux (1990) a solution is described, and details of the method can be found there. However, it is worth summarizing here the main features of the procedure.

First ψ_1 is assumed to be of the form

$$\psi_1 = \tilde{\phi}_0(y,t)\,\mathrm{e}^{\mathrm{i}\alpha x} + \text{c.c.} \tag{36}$$

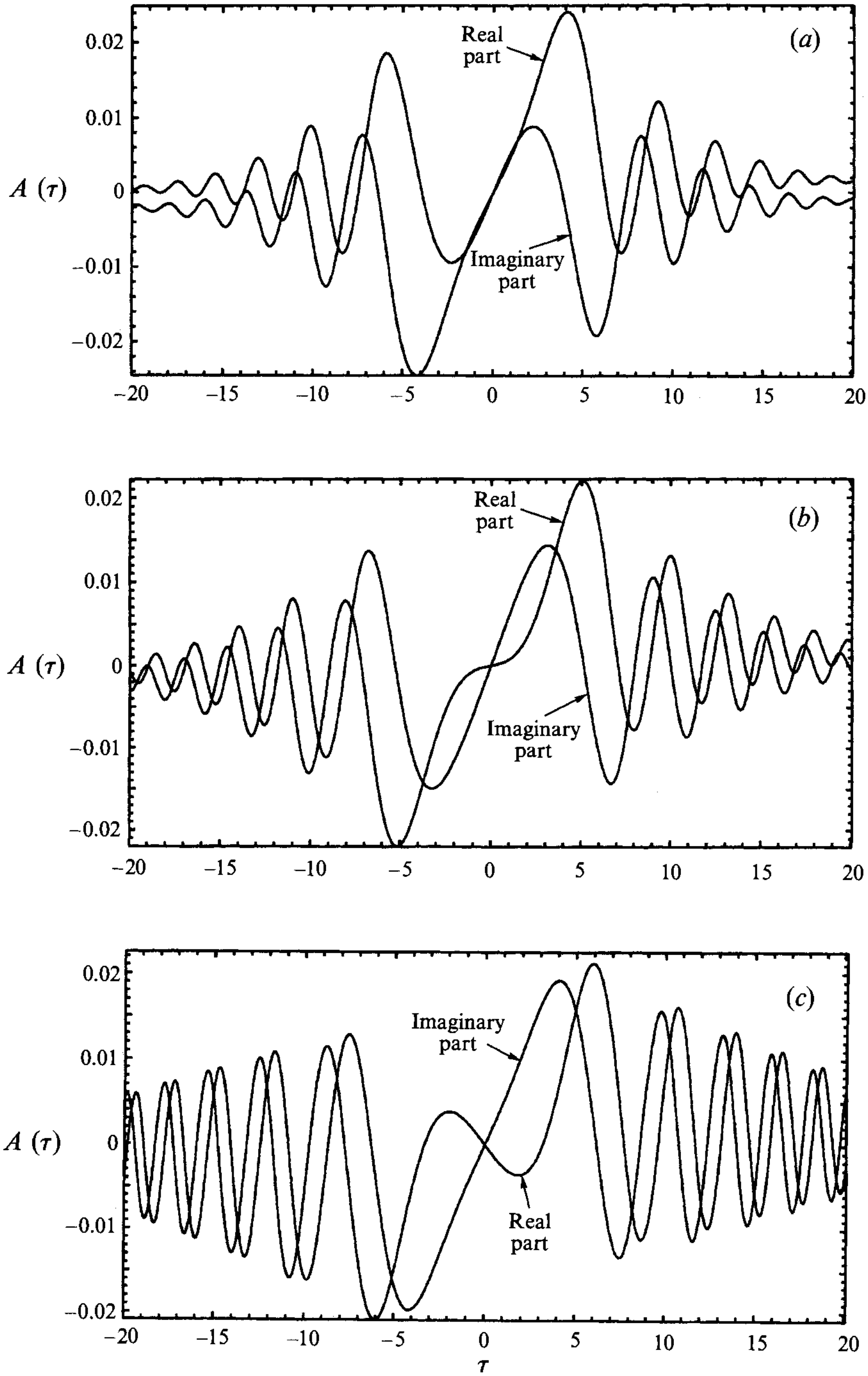

FIGURE 7. Time development of the amplitude function $A(\tau)$ for (*a*) $R_\delta = 110$, (*b*) $R_\delta = 120$, (*c*) $R_\delta = 130$.

Secondly the unknown function $\tilde{\phi}_0(y,t)$ is developed in a Fourier series of time

$$\tilde{\phi}_0 = \sum_{m=-\infty}^{+\infty} G_m(y)\,\mathrm{e}^{\mathrm{i}mt}. \tag{37}$$

Substituting from (36) and (37) into the partial differential equation (9), an infinite set of ordinary differential equations for the coefficient G_m is obtained. The structure of the solution can be found with an argument similar to that leading to (18):

$$\begin{aligned} G_m(y) = \sum_{n=-\infty}^{+\infty} \Big\{ & a_n \sum_{j=0}^{\infty} \lambda_{nmj} \exp[-[\alpha+(m-n)\mathrm{i}+j)]\,y] \\ & +(1-\delta_{n0})\, b_n \sum_{j=0}^{\infty} \theta_{nmj} \exp[-[\sigma_n+(m-n)\mathrm{i}+j]\,y] \Big\} \\ & + b_0 \sum_{j=0}^{\infty} \{\beta_{mj} \exp[-[\alpha+m\mathrm{i}+j]\,y] + \gamma_{mj}\, y \exp[-[\alpha+m\mathrm{i}+j]\,y]\}, \end{aligned} \tag{38}$$

where $$\sigma_n = (\alpha^2+2n\mathrm{i})^{\frac{1}{2}}.$$

The constants $\lambda_{nmj}, \theta_{nmj}, \beta_{mj}, \gamma_{mj}$ are given by recurrence relationships somewhat similar to (19) and the constants a_n, b_n are determined by imposing the boundary conditions at $y = 0$ after truncating the expansion (37) at the Mth term.

In figure 8 the function $\tilde{\phi}_0$ at $y = 3$ is plotted versus time for $R_\delta = 100$ and different values of α. It can be seen that, in accordance with the multiple-timescale approach previously described, the stream function around resonance is characterized by large and rapid fluctuations which damp far from t_r. Moreover, resonance is smoothed rapidly when values of α smaller than α_r are considered while it persists longer when α is larger than α_r. No qualitative difference can be observed for different values of R_δ and in particular when R_δ is larger than 138, when only the approach by Blondeaux (1990) can be applied.

Unfortunately the approach described in Blondeaux (1990) becomes computationally heavy with increasing R_δ and finally a numerical procedure should be used for R_δ larger than about 200.

4.2. *The numerical approach*

The solution of the problem (9)–(11) can be found numerically by means of an approach similar to that described in Blondeaux & Vittori (1991 *a*). Because of the use of a numerical procedure, the effects of the nonlinear terms can also be taken into account by tackling the problem posed by (4)–(6) which reduces to (9)–(11) when small values of ϵ are considered. Moreover arbitrary values of R_δ can be considered. First, let us adopt a coordinate system $(\tilde{x}, \tilde{y})$ that moves with the bottom

$$\tilde{x} = x - \frac{R_\delta}{2}\int_0^t \left(\frac{\mathrm{e}^{\mathrm{i}t}+\mathrm{c.c.}}{2}\right)\mathrm{d}t, \quad \tilde{y} = y, \tag{39}$$

and introduce a new stream function

$$\tilde{\psi} = \psi - y\tfrac{1}{2}(\mathrm{e}^{\mathrm{i}t}+\mathrm{c.c.}). \tag{40}$$

The problem is thus reduced to the equivalent problem of determining the flow induced close to a fixed wavy wall by the harmonic oscillation of the fluid far from it. Let us then consider a wall profile $\tilde{y} = F(\tilde{x}, t)$ described by

$$\tilde{y} = \sum_{n=0}^{\infty} a_n \cos(n\alpha\xi-\varphi_n), \quad \xi = \tilde{x} + \sum_{n=0}^{\infty} a_n \sin(n\alpha\xi-\varphi_n), \tag{41}$$

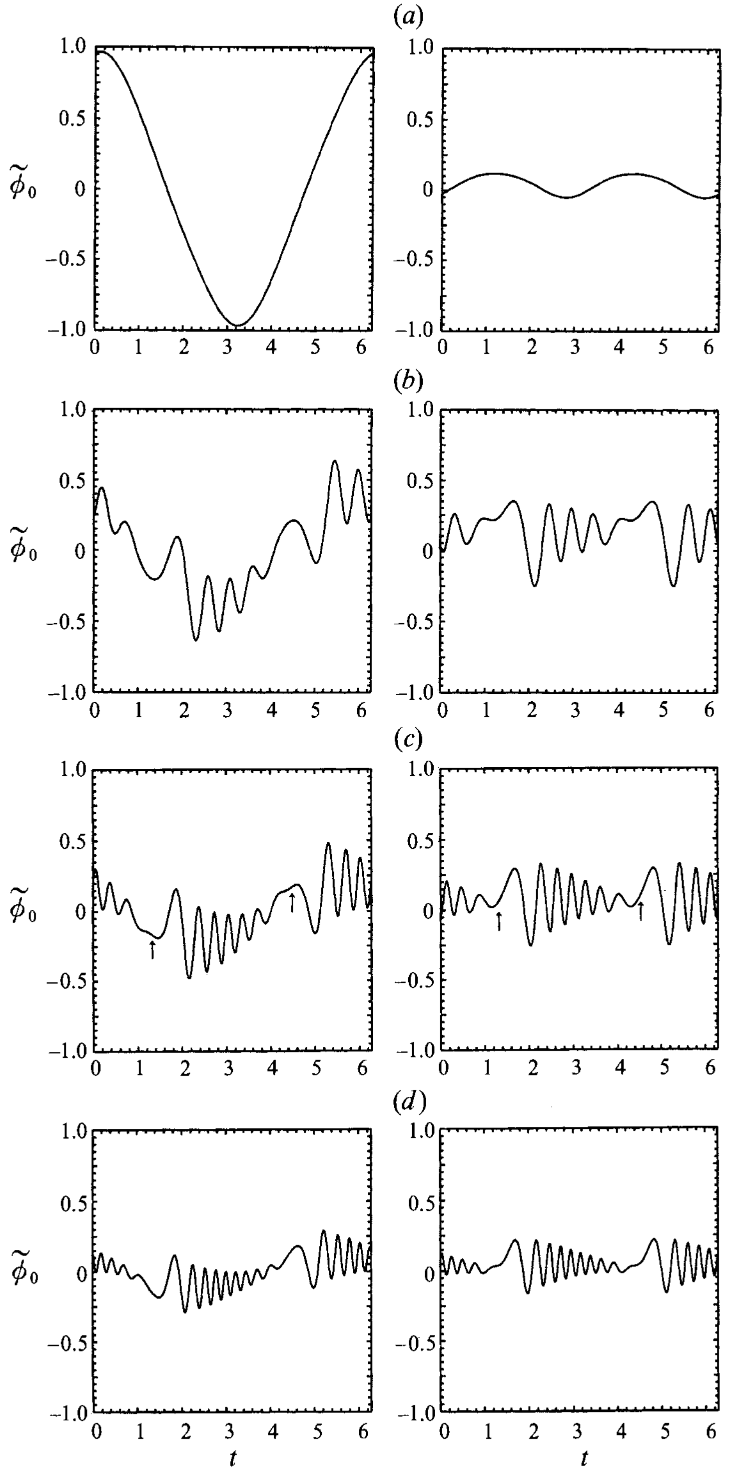

FIGURE 8. Time development of $\tilde{\phi}_0$ at $y = 3$ for $R_\delta = 100$ and (*a*) $\alpha = 0.05$; (*b*) $\alpha = 0.25$; (*c*) $\alpha = 0.395$; (*d*) $\alpha = 0.55$. Left-hand plots: real part; right-hand plots: imaginary part. $\alpha_r \approx 0.395$. Arrows denote resonance instants.

where ξ is a dummy variable. It can be easily verified that, with a proper choice of the constants a_n, φ_n, (41) can be used to describe a sinusoidal wall of small amplitude ϵ with an arbitrary degree of accuracy. To determine $\tilde{\psi}$ it is useful to introduce a new orthogonal coordinate system (ξ, η) defined by

$$\eta = \tilde{y} - \sum_{n=0}^{\infty} a_n \mathrm{e}^{-n\alpha\eta} \cos(n\alpha\xi - \varphi_n), \quad \xi = \tilde{x} + \sum_{n=0}^{\infty} a_n e^{\mathrm{i}\alpha\eta} \sin(n\alpha\xi - \varphi_n), \tag{42}$$

which maps the bottom profile into the line $\eta = 0$. Substitution of (39)–(42) into (4)–(6) leads to the following partial differential problem:

$$\frac{\partial\tilde{\omega}}{\partial t} + \frac{R_\delta}{2J}\left[\frac{\partial\tilde{\psi}}{\partial\eta}\frac{\partial\tilde{\omega}}{\partial\xi} - \frac{\partial\tilde{\psi}}{\partial\xi}\frac{\partial\tilde{\omega}}{\partial\eta}\right] = \frac{1}{2J}\left[\frac{\partial^2\tilde{\omega}}{\partial\xi^2} + \frac{\partial^2\tilde{\omega}}{\partial\eta^2}\right], \tag{43}$$

$$\frac{\partial^2\tilde{\psi}}{\partial\xi^2} + \frac{\partial^2\tilde{\psi}}{\partial\eta^2} = -J\tilde{\omega}, \tag{44}$$

$$\frac{\partial\tilde{\psi}}{\partial\xi} = \frac{\partial\tilde{\psi}}{\partial\eta} = 0 \quad \text{at} \quad \eta = 0, \tag{45}$$

$$\frac{\partial\tilde{\psi}}{\partial\xi} \rightarrow 0, \quad \frac{\partial\tilde{\psi}}{\partial\eta} \rightarrow -\cos(t) \quad \text{for} \quad \eta \rightarrow \infty, \tag{46}$$

where J is the Jacobian of transformation (42):

$$J = 1 - 2\sum_{n=0}^{\infty} n\alpha a_n \mathrm{e}^{-n\alpha\eta}\cos(n\alpha\xi - \varphi_n) + \left[\sum_{n=0}^{\infty} n\alpha a_n \mathrm{e}^{-n\alpha\eta}\cos(n\alpha\xi - \varphi_n)\right]^2 + \left[\sum_{n=0}^{\infty} n\alpha a_n \mathrm{e}^{-n\alpha\eta}\sin(n\alpha\xi - \varphi_n)\right]^2. \tag{47}$$

The problem formulated above can be solved numerically following the procedure described in Blondeaux & Vittori (1991*a*) which makes use of spectral methods and finite-difference approximations. First, the values assumed within a wavelength by the stream function $\tilde{\psi}(\xi, \eta, t)$ and the vorticity $\tilde{\omega}(\xi, \eta, t)$ on a regular grid in the ξ-direction are considered:

$$\tilde{\psi}_j(\eta, t) = \tilde{\psi}\left(\frac{jl}{N_2}, \eta, t\right), \quad \tilde{\omega}_j(\eta, t) = \tilde{\omega}\left(\frac{jl}{N_2}, \eta, t\right), \quad j = 1, 2, \ldots, N_2. \tag{48}$$

Then the discrete Fourier coefficients are introduced (Orszag 1971)

$$\left.\begin{aligned} \tilde{\psi}_j(\eta, t) &= \sum_{n=0}^{N_2-1} \tilde{\Psi}_n(\eta, t)\,\mathrm{e}^{\mathrm{i}2\pi n(j/N_2)}, \\ \tilde{\omega}_j(\eta, t) &= \sum_{n=0}^{N_2-1} \tilde{\Omega}_n(\eta, t)\,\mathrm{e}^{\mathrm{i}2\pi n(j/N_2)}, \end{aligned}\right\} \quad j = 1, 2, \ldots, N_2. \tag{49}$$

System (43)–(46) is thus reduced to a time-dependent boundary-value problem in the variable η where the unknowns are given by the functions $\tilde{\Psi}_n, \tilde{\Omega}_n$ and which is amenable to a classic computational approach. More details can be found in Blondeaux & Vittori (1991*a*). Numerical experiments have been performed to choose the characteristics of the numerical grid and to test the accuracy of the results obtained, which turn out to be affected by a relative error always smaller than 0.01. In all the simulations the fluid is at rest till $t = \frac{1}{2}\pi$ and then the oscillatory flow from the wall

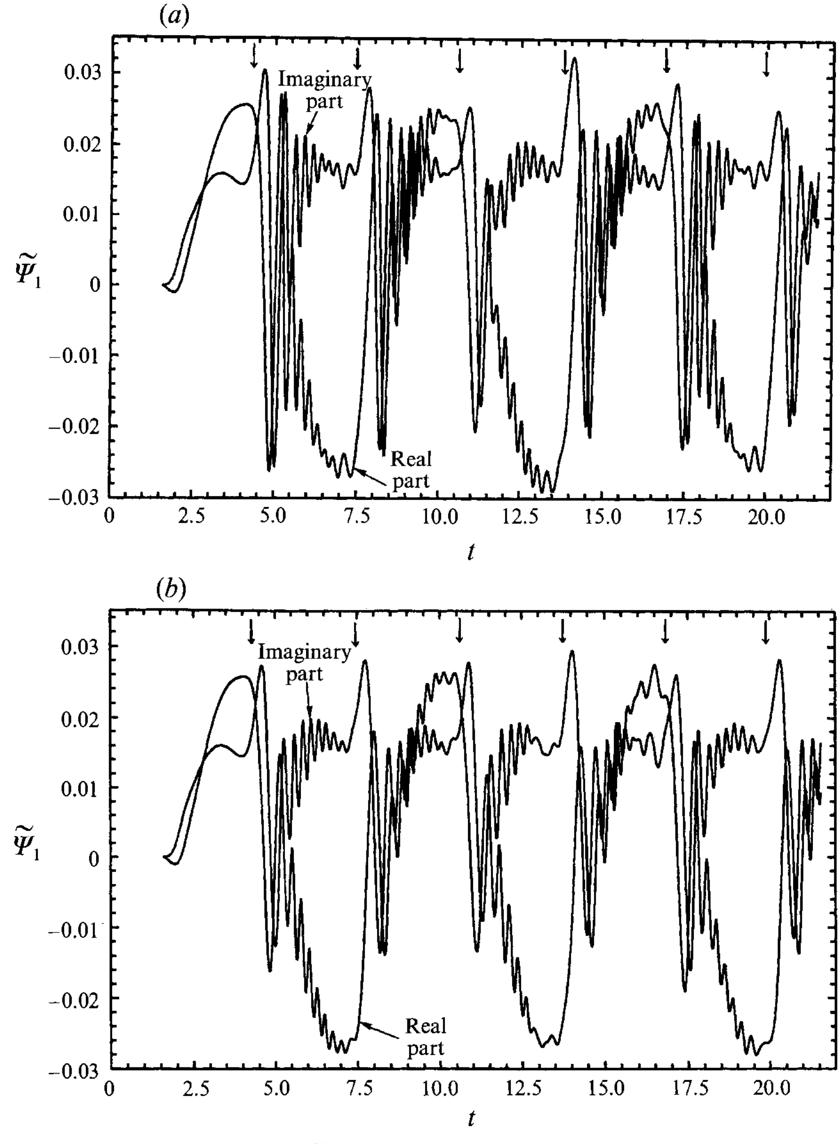

FIGURE 9. Time development of $\tilde{\Psi}_1$ at $\eta = 1.0$ for $R_\delta = 400$, $\alpha = 0.122$ and $\epsilon = 0.125$. (*a*) $N_2 = 4$, (*b*) $N_2 = 16$. Arrows denote resonance instants.

starts. The flow is always observed to evolve in a 'regime' configuration which depends on the values of the parameters (namely $\epsilon, \alpha, R_\delta$). For small values of ϵ and R_δ, when α is of order one, the attractor turns out to be a limit cycle. On increasing R_δ the flow turns out to be aperiodic. However, the characteristics of the attractor have not been determined because of the high computational costs (Blondeaux & Vittori 1991*b*).

The time development of Ψ_1 at $\eta = 1$ is shown for $R_\delta = 400$, $\alpha = \alpha_r = 0.122$ and $\epsilon = 0.125$, in figure 9. In figure 9(*a*) the solution has been obtained by setting $N_2 = 4$, while figure 9(*b*) shows the results obtained with $N_2 = 16$. The numerical solution of the problem (4)–(6) for $N_2 = 4$ corresponds to the numerical solution of the problem posed by (9)–(13), i.e. to the solution of the linear problem. On the other hand the solution for $N_2 = 16$ takes into account nonlinear effects. By comparing figures 9(*a*) and 9(*b*), it appears that (i) resonance is damped by the local acceleration term since the solution shown in figure 9(*a*) is characterized by a finite time development even though it has been obtained by neglecting nonlinear effects; (ii) for sufficiently small values of ϵ, nonlinear effects are negligible. Indeed even when $\epsilon = 0.125$, the solutions for $N_2 = 4$ and $N_2 = 16$ are almost coincident. The differences between the $N_2 = 4$ and $N_2 = 16$ cases increase for increasing values of ϵ even though they remain of small amplitude, if ϵ does not become too large. The number of superharmonic components necessary to describe the solution with sufficient accuracy depends on the parameters of the problem, namely $R_\delta, \alpha, \epsilon$. For the values of the parameters shown in figure 9, a value of N_2 equal to 16 gives sufficient accuracy. Indeed the solution obtained by setting $N_2 = 32$ is coincident with that plotted in figure 9(*b*). As expected, the solution is characterized by large and rapid fluctuations that appear at fixed time within a cycle and then damp.

When smaller values of α are considered, the amplitude of the fluctuations decreases (see figure 10*a*). In fact the parameters depart from the set that produces resonance and the solution tends to become of order ϵ and to be smooth. On the other hand when values of α larger than α_r are considered the amplitude of the fluctuations increases (see figure 10*b*). This unexpected finding is due to the excitation of free modes, which grow during the unstable time intervals as predicted by Blondeaux & Seminara (1979). Indeed the numerical solution involves both the forced response of the flow to the wall waviness and the time development of free modes. The latter, in the case of a wavy wall, are continuously exited because of the presence of the external forcing. Thus it turns out that free modes, which are momentarily unstable, explode every half-cycle even though they are stable on the average as predicted by Hall (1978). By increasing α, the fluctuations of the solution are larger than those at resonance, even though the forced component should be smaller. It is worth pointing out that for $R_\delta = 400$, the unstable wavenumbers were found by Blondeaux & Seminara (1979) to fall in a large range centred around $\alpha_c = 0.5$ and instability takes place at flow reversal. Thus for $R_\delta = 400$, the perturbations characterized by $\alpha = 0.04$ are less unstable than those characterized by $\alpha = 0.24$. The growth of free modes also provides an explanation of the aperiodic character of the flow detectable in figures 9 and 10(*b*). In fact the explosion of flow perturbations within the unstable parts of the cycle leads to different values of the stream function at every half-cycle, because the initial values of the perturbations change every half-cycle due to numerical and truncation errors. Very small differences in the initial conditions amplify because of the flow instability. The mechanism that sometimes leads the present flow to an aperiodic time behaviour is thus different from that which causes the chaotic time development of the oscillatory flow over a large-amplitude wavy wall detected by Blondeaux & Vittori (1991*b*). In the latter case, the chaotic behaviour is present even at moderate values of the Reynolds number and of course is produced by the presence of the nonlinear terms, i.e. it is due to the nonlinear interaction of the large vortex structures generated by flow separation at the crests of the wall waviness. On the other hand the present results show an aperiodic stream function even in the linear case, i.e. for very small wall amplitudes, when flow separation is absent.

No qualitative differences in the solution can be observed as R_δ changes, except for the disappearance of the aperiodic behaviour when small values of R_δ are considered. In fact on decreasing R_δ the flow becomes stable and only the forced mode is given by the numerical solution.

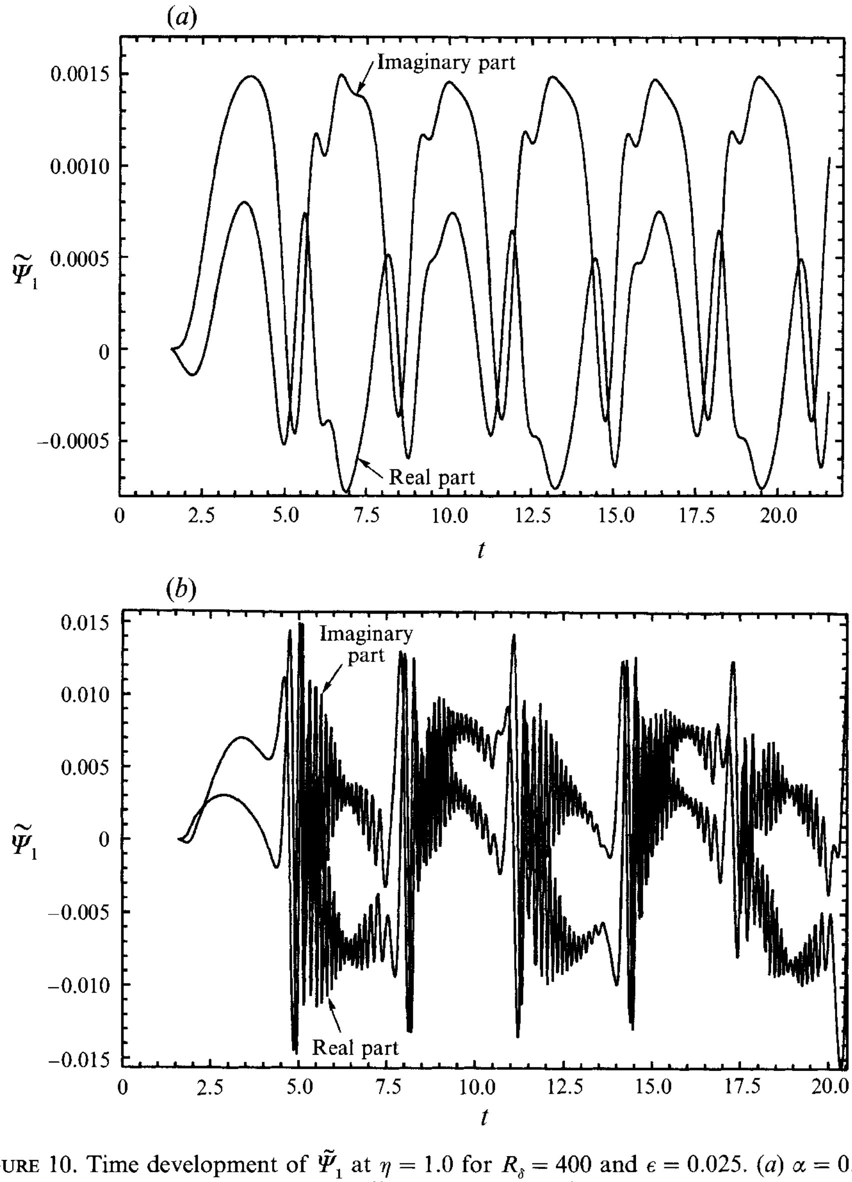

FIGURE 10. Time development of $\tilde{\Psi}_1$ at $\eta = 1.0$ for $R_\delta = 400$ and $\epsilon = 0.025$. (*a*) $\alpha = 0.04$ ($N_2 = 4$), (*b*) $\alpha = 0.24$ ($N_2 = 4$).

5. Conclusions

Modifications induced to the structure of the Stokes boundary layer by wall imperfections have been studied when the amplitude of the wall imperfections is much smaller than the boundary-layer thickness and for large values of R_δ.

The present results, along with those derived on the basis of a linear stability analyses by Hall (1978) and Blondeaux & Seminara (1979), the three-dimensional numerical simulations performed by Akhavan *et al.* (1991) and the recent theoretical findings by Wu (1992), suggest some speculations on a possible route to turbulence in Stokes layers.

The numerical calculations by Akhavan *et al.* (1991) and the nonlinear stability analysis by Wu (1992) seem to suggest that the turbulence bursts observed in flat Stokes

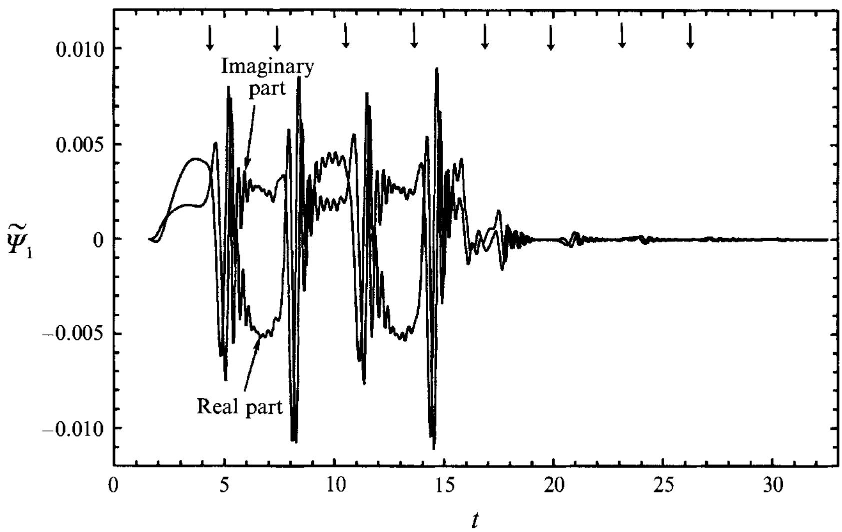

FIGURE 11. Time development of $\tilde{\Psi}_1$ at $\eta = 1.0$ for $R_\delta = 400$, $\alpha = 0.122$. For t smaller than 15.85: $a_1 = 0.04$, $\varphi_1 = 0$, $a_2 = -0.04$, $\varphi_2 = 0$, $a_3 = 0.04$, $\varphi_3 = \pi/2$, $a_4 = -0.04$, $\varphi_4 = \pi/2$ and other $a_n = 0$. For t larger than 15.85 all a_n vanish. Arrows denote resonance instants.

boundary layers during the decelerating parts of the cycle are produced by the growth of three-dimensional disturbances interacting with two-dimensional waves. While no justification is provided in the work by Akhavan *et al.* (1991) for the pre-existence of the two-dimensional finite-amplitude waves, in the paper of Wu (1992) the growth of the two-dimensional component is shown to be caused by its interaction with the three-dimensional waves. In both cases however, the three-dimensional character of flow perturbation is essential. One of the referees pointed out that Wu & Cowley (1994), in an as yet unpublished paper, have shown that interacting two-dimensional modes can also develop a finite time singularity and attain a finite value.

In the present contribution the existence of another possible mechanism triggering transition to turbulence in a Stokes layer is discussed. Indeed wall imperfections are shown to cause the presence of large two-dimensional waves which, triggering the instantaneous growth of two-dimensional free modes, produce a bursting flow with many characteristics in common with the experimental observations. The appearance of a 'bursting turbulent' flow in the two-dimensional Stokes boundary layer over a wavy wall and the key role played by wall imperfections is shown in figure 11 where the time development of $\tilde{\Psi}_1$ is plotted for $R_\delta = 400$. For t smaller than 15.85 the wall is wavy with a waviness characterized by many spatial components. For t larger than 15.85 wall imperfections have been removed, hence the wall is perfectly flat. Within the time range 1.57–15.85, i.e. after the start of the fluid motion and before the removal of the wall waviness, the flow is characterized by bursts of 'turbulence'. During the decelerating parts of the cycle, wall imperfetions cause transition to turbulence by triggering the instantaneous growth of two-dimensional free modes through the intermediary of the forced mode. However, during the accelerating parts of the cycle the perturbations tend to be damped and the flow tends to relaminarize. This may be the reason why a clear limit between the laminar and the turbulent regimes has not been detected by experimental investigations.

The overall stability of the Stokes flow over a flat wall with respect to two-dimensional perturbations is also evident in figure 11. Indeed after the removal of the wall waviness, i.e. for the flat-wall case, the initial perturbations tends to decay, even though there are parts of the cycle during which it amplifies, and after few cycles the flow has recovered its full laminar character.

The financial support by 'Ministero dell'Università e della Ricerca Scientifica e Tecnologica' and the Commission of the European Communities, Directorate General for Science, Research and Development, under contract n. MAS2-CT92-0027 is acknowledged.

Appendix

We show that keeping the viscous $O(R_\delta^{-1})$ term in (14) is equivalent to a formal matched asymptotic expansion approach where viscous effects turn out to have the same order of magnitude as convective terms in 'critical' layers of thickness $O(R_\delta^{-\frac{1}{3}})$ adjacent to the wall and located at distances y such that the quantity $(\partial\psi_0/\partial y - u(t))$ tends to vanish. For convenience let us consider values of t close to zero in such a way that only the viscous critical layer close to the wall exists.

For large values of R_δ in a region of y of $O(1)$, the unknown function ψ_1 can be expanded in powers of the small parameter $(R_\delta)^{-1}$ in the form

$$\psi_1^{(0)}(x,y,t) = R_\delta^C[\phi_0^{(0)}(y,t) + O(R_\delta^{-1})]\,P(t)\,\mathrm{e}^{i\alpha x} + \text{c.c.}, \tag{A 1}$$

where C is unknown at this stage.

Substituting from (A 1) into (9) and equating like powers of $(R_\delta)^{-1}$, at the leading order of approximation the following equation is obtained:

$$\mathrm{i}\alpha\left(\frac{\partial\psi_0}{\partial y} - u\right)\mathrm{N}^2\phi_0^{(0)} - \mathrm{i}\alpha\phi_0^{(0)}\frac{\partial^3\psi_0}{\partial y^3} = 0. \tag{A 2}$$

Following a procedure similar to that previously used, it can be shown that the solution satisfying boundary conditions (11) is

$$\phi_0^{(0)} = \sum_{n=0}^{\infty}\sum_{m=0}^{n} f_{nm}(t)\exp\{-[\alpha + n(1+\mathrm{i}) - 2\mathrm{i}m]\,y\}, \tag{A 3}$$

where the coefficients $f_{nm}(t)$ are provided by the recursive relationship

$$\begin{aligned} f_{n,m} = {} & \{\tfrac{1}{2}\mathrm{e}^{\mathrm{i}t}\lambda_1[(\alpha + (n-1)(1+\mathrm{i}) - 2\mathrm{i}m)^2 - \alpha^2 - 2\mathrm{i}]f_{n-1,m} \\ & + \tfrac{1}{2}\mathrm{e}^{-\mathrm{i}t}\lambda_2[(\alpha + (n-1)(1+\mathrm{i}) - 2\mathrm{i}(m-1))^2 - \alpha^2 + 2\mathrm{i}]f_{n-1,m-1}\}/ \\ & \{u(t)\,[(\alpha + n(1+\mathrm{i}) - 2\mathrm{i}m)^2 - \alpha^2]\}, \end{aligned} \tag{A 4}$$

$$\lambda_1 = \begin{cases} 0, & m = n \\ 1, & 0 \leqslant m \leqslant n-1, \end{cases} \qquad \lambda_2 = \begin{cases} 0, & m = 0 \\ 1, & 1 \leqslant m \leqslant n. \end{cases}$$

The unknown constant $f_{0,0}$ cannot be determined in such a way as to satisfy both (10*a*) and (10*b*). The existence of a viscous layer close to the wall is thus inferred. A balance between the order of magnitude of convective and viscous terms suggests that the thickness of the viscous layer is $O(R_\delta^{-\frac{1}{3}})$.

Let us then define $\eta = R_\delta^{\frac{1}{3}}y$ and assume that the unknown function ψ_1 in the inner layer is provided by the expansion

$$\psi_1^{(i)} = [R_\delta^{-\frac{1}{3}}\phi_0^{(i)} + O(R_\delta^{-\frac{2}{3}})]\,P(t)\,\mathrm{e}^{\mathrm{i}\alpha x} + \text{c.c.}, \tag{A 5}$$

where the order of magnitude of $\psi_1^{(i)}$ is forced by the boundary condition (10*b*).

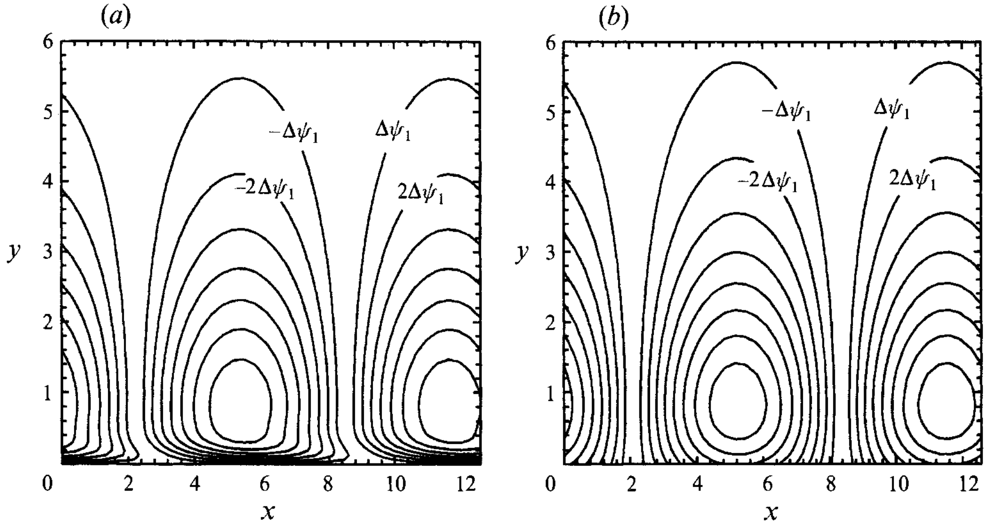

FIGURE 12. Spatial structure of the correction to the stream function induced by a wall waviness in Stokes flow ($\psi_1(x,y,t)$): $R_\delta = 500$, $\alpha = 0.5$, $t = 0$. Outer region, $O(y) = 1$. (*a*) Equation (18), (*b*) equation (A 3) ($\Delta\psi_1 = 0.04$).

At the leading order of approximation, (9) and boundary conditions (10) give rise to the following problem for $\phi_0^{(i)}$:

$$\frac{\partial^4 \phi_0^{(i)}}{\partial \eta^4} + \mathrm{i}\alpha\eta G(t)\frac{\partial^2 \phi_0^{(i)}}{\partial \eta^2} = 0, \tag{A 6}$$

$$\phi_0^{(i)} = 0, \quad \frac{\partial \phi_0^{(i)}}{\partial \eta} = G(t) \quad \text{at} \quad \eta = 0, \tag{A 7a, b}$$

where
$$G(t) = \tfrac{1}{2}(1+\mathrm{i})\,\mathrm{e}^{\mathrm{i}t} + \text{c.c.} \tag{A 8}$$

Moreover it should be remembered that $\phi_0^{(i)}$ for η tending to infinity should match $\phi_0^{(0)}$ for y tending to zero.

Defining $w = (\mathrm{i}\alpha G(t))^{\frac{1}{3}}\eta$ and after some algebra, the Airy equation is obtained and the solution of (A 6) can be easily found to be

$$\phi_0^{(i)} = a + bw + c\int_0^w \mathrm{d}u \int_0^u \mathrm{Ai}(-v)\,\mathrm{d}v + g\int_0^w \mathrm{d}u \int_0^u \mathrm{Bi}(-v)\,\mathrm{d}v, \tag{A 9}$$

where Ai and Bi are Airy functions.

Boundary conditions (A 7*a, b*) force

$$a = 0, \quad b = (\mathrm{i}\alpha)^{-\frac{1}{3}} G(t)^{\frac{2}{3}}. \tag{A 10}$$

The matching of the limiting form (A 9) as $w \to \infty$ with (A 3) as $y \to \infty$ gives the values of c and g in the form

$$c = -\tfrac{3}{2}(\mathrm{i}\alpha)^{-\frac{1}{3}} G^{\frac{2}{3}}, \tag{A 11}$$

$$\left.\begin{aligned} g &= \frac{\mathrm{i}-1}{\mathrm{i}+1}c, \quad 0 \leqslant \arg(\mathrm{i}G)^{\frac{1}{2}} < \pi, \\ g &= \frac{\mathrm{i}+1}{\mathrm{i}-1}c, \quad \pi \leqslant \arg(\mathrm{i}G)^{\frac{1}{2}} < 2\pi. \end{aligned}\right\} \tag{A 12}$$

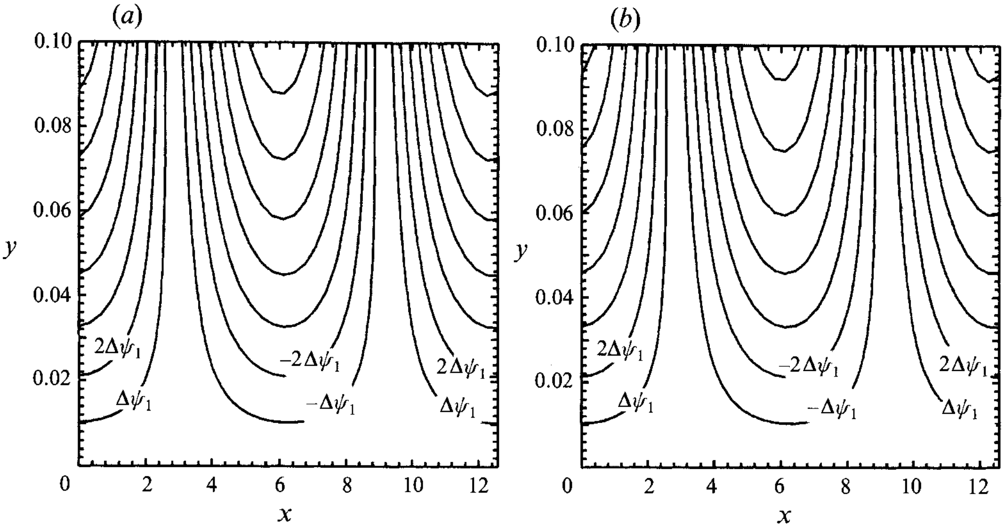

FIGURE 13. As figure 12 but for the inner region, $O(y) = R_\delta^{-\frac{1}{3}}$. (*a*) Equation (18), (*b*) equation (A 9) ($\Delta\psi_1 = 0.02$).

Furthermore $f_{0,0}$ is forced to be

$$f_{0,0} = \left[-\frac{c}{3^{\frac{1}{3}}\Gamma(\frac{1}{3})} + \frac{g3^{\frac{1}{6}}}{\Gamma(\frac{1}{3})}\right]\left[\sum_{n=0}^{\infty}\sum_{m=0}^{n}(f_{n,m}/f_{0,0})\right]^{-1}, \tag{A 13}$$

with the exponent C set to $-\frac{1}{3}$.

Having an outer expansion valid in the outer region and an inner expansion valid in the inner region, we can form a single composite expansion which is uniformly valid throughout the whole flow field.

Figures 12 and 13 show a comparison between (18) and the asymptotic solution just described. The two solutions are found to be practically coincident (similar results are obtained for different values of the parameter). It may be useful to point out that the term $(2/R_\delta)(\partial/\partial t)(\mathrm{N}^2\phi_1)$ has been correctly neglected in (14), as it is negligible both in the inviscid and in the viscous region.

As previously pointed out a similar analysis applies for arbitrary values of t but considering the existence of other critical layers.

REFERENCES

AKHAVAN, R., KAMM, R. D. & SHAPIRO, A. H. 1991 An investigation of transition to turbulence in bounded oscillatory Stokes flows. Part 2. Numerical simulations. *J. Fluid Mech.* **225**, 423–444.

BAYLY, B. J. 1986 Three-dimensional instability of elliptical flow. *Phys. Rev. Lett.* **57**, 2160–2163.

BAYLY, B. J., ORSZAG, S. A. & HERBERT, T. 1988 Instability mechanisms in shear-flow transition. *Ann. Rev. Fluid Mech.* **20**, 359–391.

BLONDEAUX, P. 1990 Sand ripples under sea waves. Part 1. Ripple formation. *J. Fluid Mech.* **218**, 1–17.

BLONDEAUX, P. & SEMINARA, G. 1979 Transizione incipiente al fondo di un'onda di gravità. *Rendiconti Accad. Naz. Lincei* **67**, 407–417.

BLONDEAUX, P. & VITTORI, G. 1991*a* Vorticity dynamics in an oscillatory flow over a rippled bed. *J. Fluid Mech.* **226**, 257–289.

BLONDEAUX, P. & VITTORI, G. 1991*b* A route to chaos in an oscillatory flow: Feigenbaum scenario. *Phys. Fluids* A **3**, 2492–2495.

CODDINGTON, E. A. & LEVINSON, N. 1955 *Theory of Ordinary Differential Equations.* McGraw-Hill.

CORKE, T. C., BAR SEVER, A. & MORKOVIN, M. V. 1986 Experiments on transition enhancement by distributed roughness. *Phys. Fluids* **29**, 3199–3213.

COWLEY, S. J. 1987 High frequency Rayleigh instability of Stokes layers. In *Stability of Time Dependent and Spatially Varying Flows*, (ed. D. L. Dwoyer & M. Y. Hussaini), pp. 261–275. Springer.

CROUCH, J. D. 1992 Non-localized receptivity of boundary layers. *J. Fluid Mech.* **244**, 567–581.

ECKMANN, D. M. & GROTBERG, J. B. 1991 Experiments on transition to turbulence in oscillatory pipe flow. *J. Fluid Mech.* **222**, 329–350.

GOLDSTEIN, M. E. & HULTGREN, L. S. 1989 Boundary-layer receptivity to long-wave free-stream disturbances. *Ann. Rev. Fluid Mech.* **21**, 137–166.

HALL, P. 1978 The linear stability of flat Stokes layers. *Proc. R. Soc. Lond.* A **359**, 151–166.

HARA, T. & MEI, C. C. 1990 Oscillating flows over periodic ripples. *J. Fluid Mech.* **211**, 183–209.

HINO, M., SAWAMOTO, M. & TAKASU, S. 1976 Experiments on transition to turbulence in an oscillatory pipe flow. *J. Fluid Mech.* **75**, 193–207.

KANEKO, A. & HONJII, H. 1979 Double structures of steady streaming in the oscillatory viscous flow over a wavy wall. *J. Fluid Mech.* **93**, 727–736.

KERVORKIAN, J. 1971 Passage through resonance for a one-dimensional oscillator with slowly varying frequency. *SIAM J. Appl. Maths* **20**, 364–373.

LANDMAN, M. J. & SAFFMAN, P. G. 1987 The three-dimensional instability of strained vortices in a viscous fluid. *Phys. Fluids* **30**, 2339–2342.

LI, H. 1954 Stability of oscillatory laminar flow along a wall. *US Army, Beach Erosion Board, TM* 47.

LYNE, W. H. 1971 Unsteady viscous flow over wavy wall. *J. Fluid Mech.* **50**, 33–48.

MERKLY, P. & THOMANN, H. 1975 Transition to turbulence and velocity distribution in an oscillatory pipe flow. *J. Fluid Mech.* **68**, 567–575.

MONKEVITZ, M. A. 1983 Lineare Stabilitats untersuchungen au den oszillierenden Grenzschichten von Stokes. PhD thesis 7297, Federal Institute of Technology, Zurich, Switzerland.

MONKEVITZ, M. A. & BUNSTER, A. C. 1985 The stability of the Stokes layer: visual observations and some theoretical considerations. In *Stability of Time Development and Spatially Varying Flows* (ed. D. L. Dwoyer & M. Y. Hussaini), pp. 244–260. Springer.

ORSZAG, S. A. 1971 Numerical simulation of incompressible flows within simple boundaries: accuracy. *J. Fluid Mech.* **49**, 75–112.

PIERREHUMBERT, R. T. 1986 Universal short-wave instability of two-dimensional eddies in an inviscid fluid. *Phys. Rev. Lett.* **57**, 2157–2159.

RAMAPRIAN, B. R. & MULLER, A. 1980 Transitional periodic boundary layer study. *J. Hydraul. Div ASCE* **106** (HY 12), 1956–2071.

RESHOTKO, E. 1976 Boundary layer stability and transition. *Ann. Rev. Fluid Mech.* **8**, 311–349.

RESHOTKO, E. 1984 Disturbances in a laminar boundary layer due to distributed roughness. In *Turbulence and Chaotic Phenomena in Fluids* (ed. T. Tatsumi), pp. 39–46. Elsevier.

SEMINARA, G. & HALL, P. 1975 Linear stability of slowly varying unsteady flows in a curved channel. *Proc. R. Soc. Lond.* A **346**, 279–303.

SEMINARA, G. & HALL, P. 1976 Centrifugal instability of a Stokes layer: linear theory. *Proc. R. Soc. Lond.* A **350**, 299–316.

SERGEEV, S. I. 1966 Fluid oscillations in pipes at moderate Reynolds number. *Fluid Dyn.* **1**, 121–122.

SHEN, S. F. 1961 Some considerations on the laminar stability of time dependent basic flows. *J. Aero Sci.* **28**, 397–404.

SLEATH, J. F. A. 1976 On rolling-grain ripples. *J. Hydraul. Res.* **14**, 69–81.

STOKES, G. G. 1855 On the effect of the internal friction of fluids on the motion of pendulums. *Trans. Camb. Phil. Soc.* **9**.

TROMANS, P. 1976 The stability of oscillating pipe flow. Abstract of lecture given at *Euromech 73: Oscillatory Flows in Ducts, Aix-en-Provence, April 13–15.*

VITTORI, G. 1988 Nonlinear viscous oscillatory flow over a small amplitude wavy wall. *J. Hydraul. Res.* **27**, 267–280.

Vittori, G. 1992 Oscillatory boundary layer induced by sea waves over brick-pattern ripples. *J. Hydraul. Engng* **118**, 1241–1259.

Von Kerczek, C. & Davis, S. H. 1974 Linear stability theory of oscillatory Stokes layers. *J. Fluid Mech.* **62**, 753–773.

Wu, X. 1992 The nonlinear evolution of high-frequency resonant triad waves in an oscillatory Stokes layer at high Reynolds number. *J. Fluid Mech.* **245**, 553–597.

Wu, X. & Cowley, S. J. 1994 The nonlinear evolution of high-frequency disturbances in an oscillatory Stokes layer at high Reynolds numbers. To be submitted.

Wu, X., Lee, S. S. & Cowley, S. J. 1993 On the weakly nonlinear three-dimensional instability of shear layers to pairs of oblique waves: the Stokes layer as a paradigm. *J. Fluid Mech.* **253**, 681–721.